Title: Quantum Information Processing with Spins and Topological Quantum Systems

Date: Nov 28, 2011 04:00 PM

URL: http://pirsa.org/11110139

Abstract: One of the major obstacles in quantum information processing is to prevent a quantum bit from decoherence. One powerful approach to protect quantum coherence is dynamical decoupling. I will present some recent progress of diamond-based quantum information processing using dynamical decoupling. The other promising approach is to use topological quantum systems, which are intrinsically insensitive to local perturbations. I will discuss some ideas to create and probe topological quantum systems. Furthermore, I will propose a hybrid platform between topological and conventional quantum systems, which can combine the advantages from both.

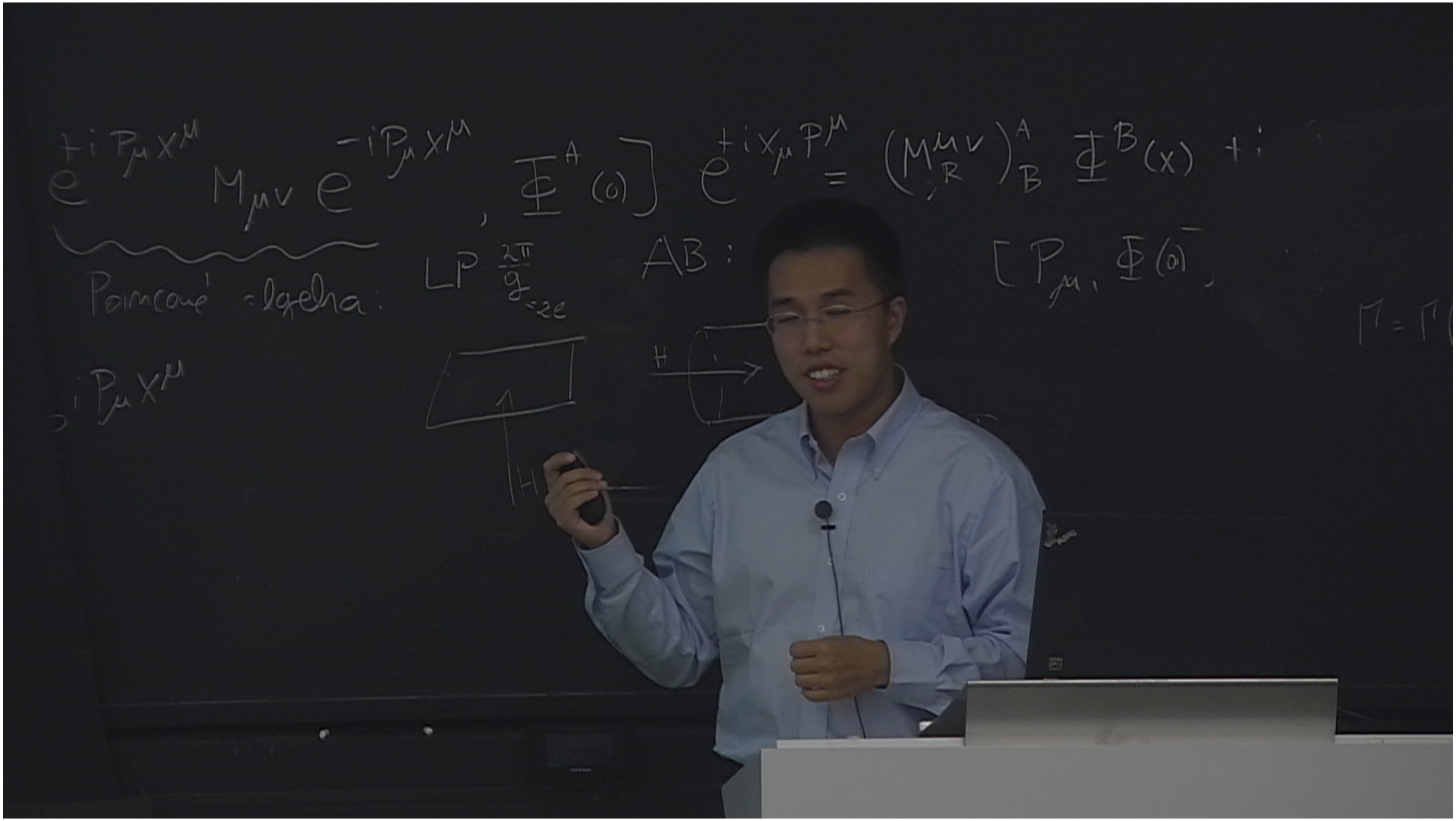

Quantum Information Processing with Spins and Topological Quantum Systems

Liang Jiang
IQI, Caltech

(Perimeter Institute, Quantum Information Seminar)

2011.11.28

Quantum Systems

1. Conventional Quantum Systems
   - E.g., spins, ions, photons, SC devices, …
   - Merits: universal gate set, distant entanglement, …
   - Challenges: vulnerable to various imperfections

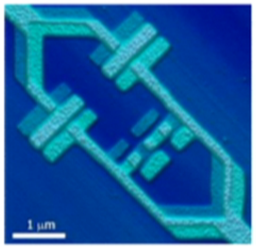

2. Topological Quantum Systems
   - E.g., Kitaev lattice model, FQHE, Topological Insulators, …
   - Merits: robust against local decoherence.
   - Challenges: non-universal, hard to build a network …

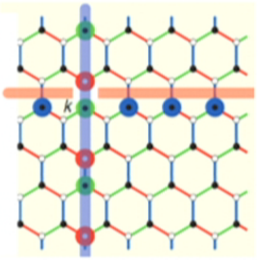

Outline

1. Spin Systems for QIP (at Room Temperature)
   - Readout of a single nuclear spin
   - Nuclear spin quantum memory
   - Quantum state transfer via thermal spin chain
2. Topological Quantum Systems for QIP
   - Majorana fermions
   - Various approaches to create & probe MFs
   - Hybrid platforms between topological and conventional quantum systems

Motivation: Quantum Money

- Encode secure information in array of solid-state qubits
- Basic Idea
  - Initialize a product state of individual qubits in arbitrary basis only known to issuer
- Advantages:
  - Impossible to copy (**no-cloning principle**)
  - Attempt to read the array by third party will leave a trace (chance to crack 2^{-N})
- Requirements
  - Solid state system and room temperature
  - High fidelity readout
  - Long coherence time

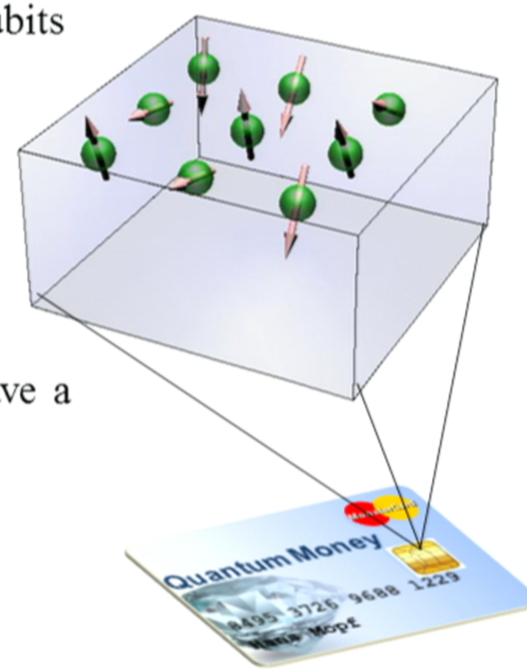

S. Wiesner. Conjugate coding. SIGACT News, 15(1):78–88, 1983.

QIP with Nuclear Magnetic Resonance

Achievements of NMR in QIP:

1. Demonstrated various quantum algorithms
   - Shor's Factorial Algorithms 15=3*5
   - Approximate Jone's polynomials …
2. Various powerful quantum control techniques
   - Spin echo
   - Dynamical decoupling

Challenges of NMR for QIP:

1. **Readout sensitivity**
2. Ensemble of nuclear spin
3. Low T & High B
4. Issue of scalability …

How to improve readout sensitivity?

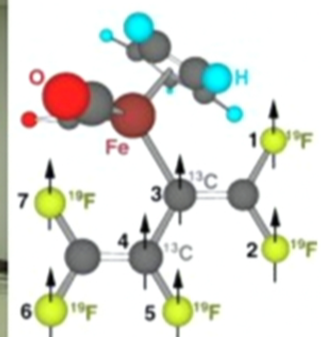

Vandersypen, Steffen, Breyta, Yannoni, Sherwood, Chuang, Nature 414, 883 (2001).
Passante, Moussa, Ryan, Laflamme, PRL 103, 250501 (2009).

Towards Sensing Single Nuclear Spin

"Replace detective coil with ultrasensitive detection technique …," with combined merits:

1. High sensitivity (Tesla/Hz)
2. High spatial resolution ($\sim 1/r^3$)

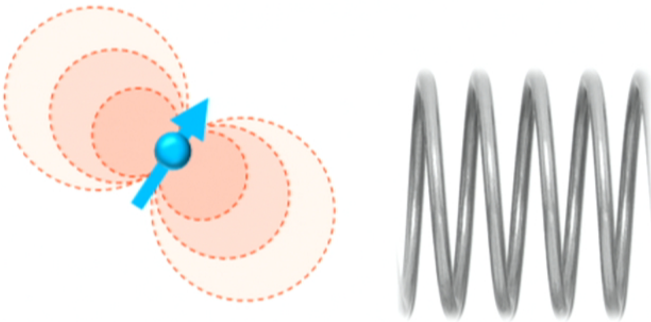

Pines & collaborators, PNAS 100, 9122 (2003)

Towards Sensing Single Nuclear Spin

"Replace detective coil with ultrasensitive detection technique …," with combined merits:

1. High sensitivity (Tesla/Hz)
2. High spatial resolution ($\sim 1/r^3$)

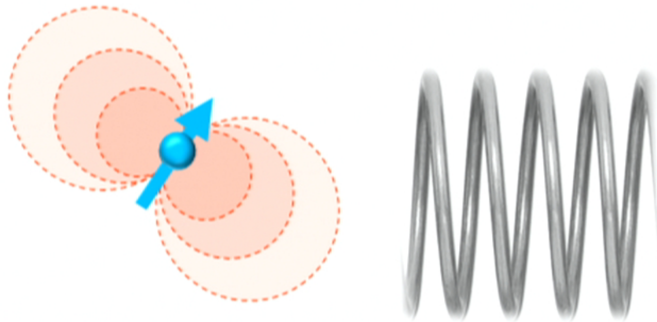

Various ultrasensitive techniques:

- Atomic vapor cell
- Hall sensor
- Force sensor
- SQUID …

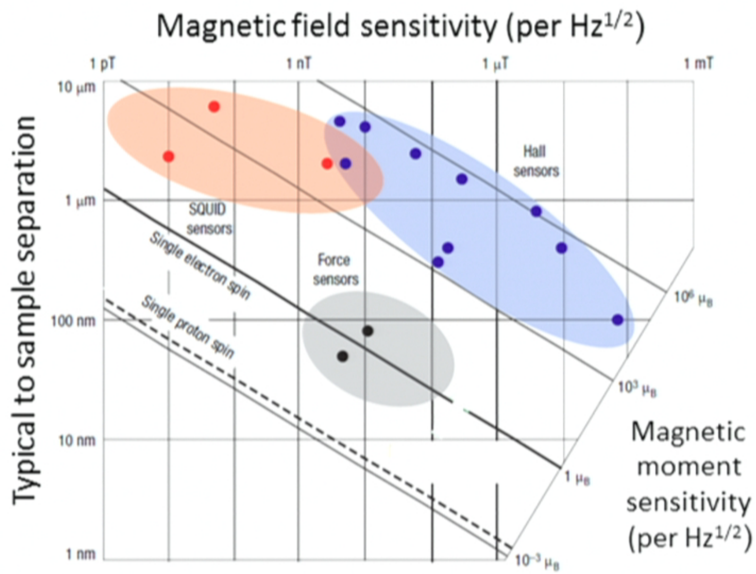

Degen, Nat Nano 3 (11), 643-644 (2008)
Pines & collaborators, PNAS 100, 9122 (2003)

Towards Sensing Single Nuclear Spin

"Replace detective coil with ultrasensitive detection technique …," with combined merits:

1. High sensitivity (Tesla/Hz)
2. High spatial resolution ($\sim 1/r^3$)

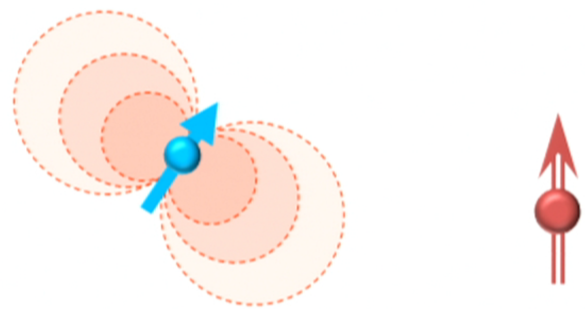

Various ultrasensitive techniques:

- Atomic vapor cell
- Hall sensor
- Force sensor
- SQUID …

Diamond spin sensor

- Large μ_B & small r

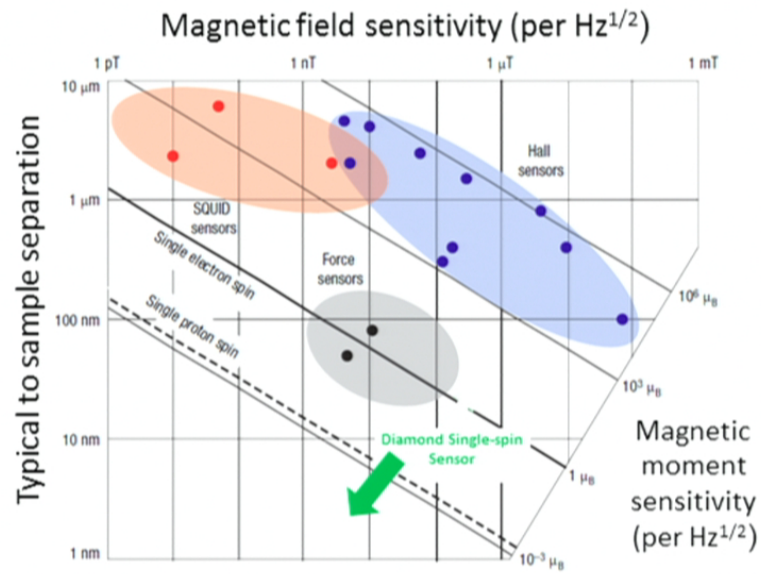

Theory: Taylor, Cappellaro, Childress, L J, et al., Nat. Phys. (2008)
Exp: Maze, Hodges, L J., et al., Nature (2008).

Degen, Nat Nano 3 (11), 643-644 (2008)
Pines & collaborators, PNAS 100, 9122 (2003)

Towards Sensing Single Nuclear Spin

"Replace detective coil with ultrasensitive detection technique ...," with combined merits:

1. High sensitivity (Tesla/Hz)
2. High spatial resolution ($\sim 1/r^3$)

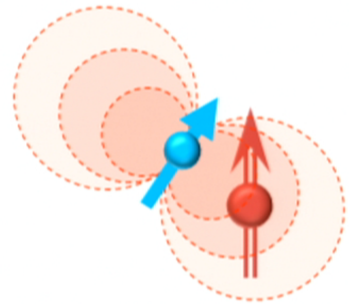

Various ultrasensitive techniques:

- Atomic vapor cell
- Hall sensor
- Force sensor
- SQUID ...

Diamond spin sensor

- Large μ_B & small r

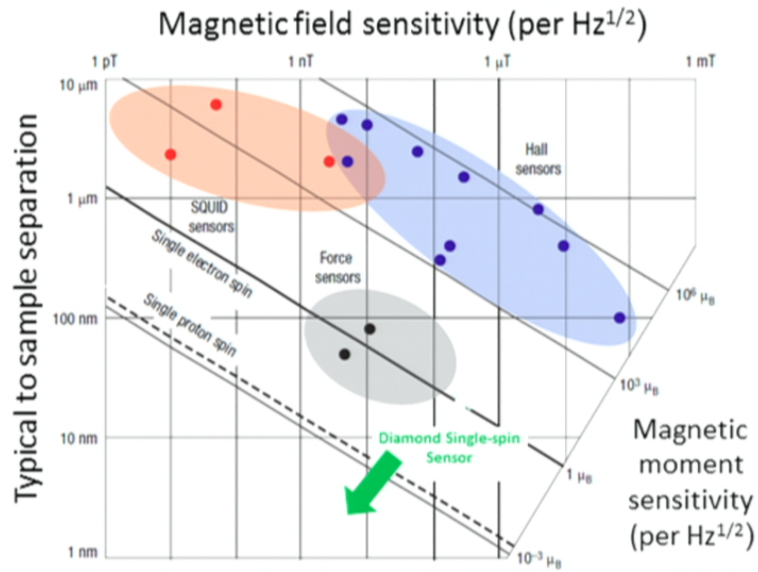

Theory: Taylor, Cappellaro, Childress, L J, et al., Nat. Phys. (2008)
Exp: Maze, Hodges, L J., et al., Nature (2008).

Degen, Nat Nano 3 (11), 643-644 (2008)
Pines & collaborators, PNAS 100, 9122 (2003)

Measure Single Nuclear Spin – the Idea

Nuclear Spin: 

Sensor Spin: 

L.J., Hodges, Maze, Maurer, Taylor, Cory, Hemmer, Walsworth, Yacoby, Zibrov, Lukin, Science 326, 267 (2009).

Measure Single Nuclear Spin – the Idea

Nuclear Spin: 

Sensor Spin: 

Suppose:

1. *Initialize sensor spin*
2. *Perform CNOT gate*
3. *Optical readout of sensor spin*

L.J., Hodges, Maze, Maurer, Taylor, Cory, Hemmer, Walsworth, Yacoby, Zibrov, Lukin, Science 326, 267 (2009).

Measure Single Nuclear Spin – the Idea

Suppose:

1. *Initialize sensor spin*
2. *Perform CNOT gate*
3. *Optical readout of sensor spin*

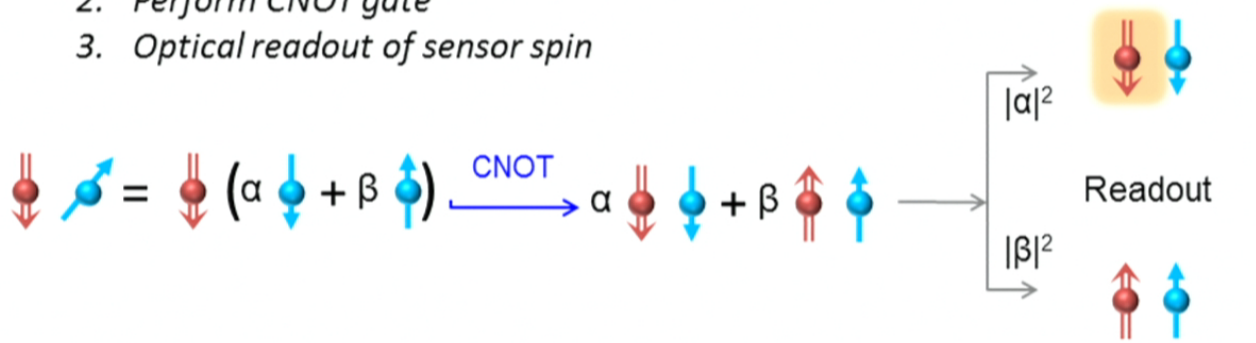

L.J., Hodges, Maze, Maurer, Taylor, Cory, Hemmer, Walsworth, Yacoby, Zibrov, Lukin, Science 326, 267 (2009).

Measure Single Nuclear Spin – the Idea

Nuclear Spin: & Sensor Spin: &

Suppose:

1. *Initialize sensor spin*
2. *Perform CNOT gate*
3. *Optical readout of sensor spin*

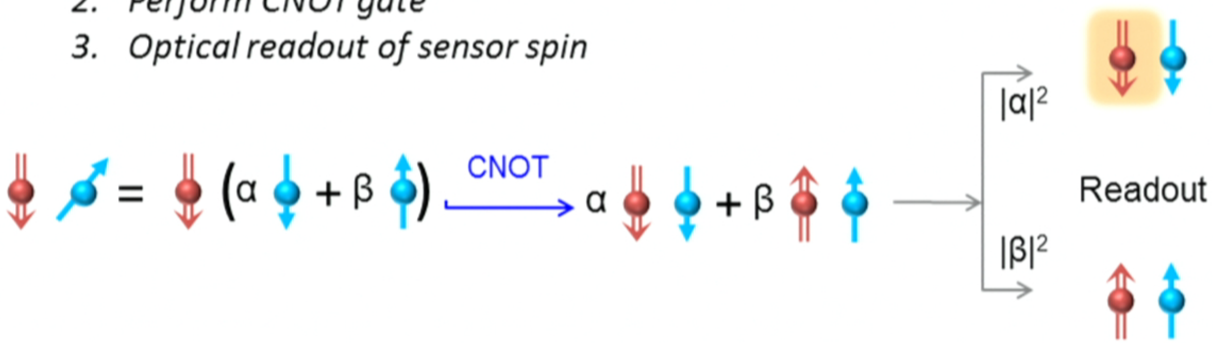

Sensor spin $|0\rangle_e$

Nuclear spin $\alpha|\downarrow\rangle_n + \beta|\uparrow\rangle_n$

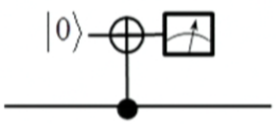

L.J., Hodges, Maze, Maurer, Taylor, Cory, Hemmer, Walsworth, Yacoby, Zibrov, Lukin, Science 326, 267 (2009).

Measure Single Nuclear Spin – the Idea

Nuclear Spin: & Sensor Spin: &

Suppose:

1. *Initialize sensor spin*
2. *Perform CNOT gate*
3. *Optical readout of sensor spin*
4. **No flip of nuclear spin**

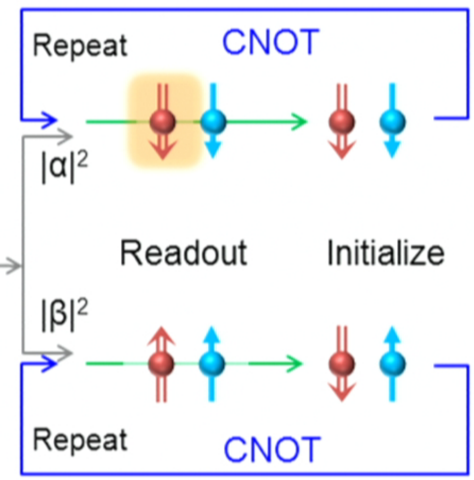

Sensor spin $|0\rangle_e$

Nuclear spin $\alpha|\downarrow\rangle_n + \beta|\uparrow\rangle_n$

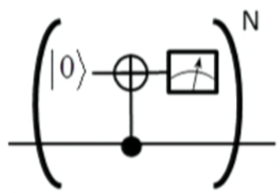

L.J., Hodges, Maze, Maurer, Taylor, Cory, Hemmer, Walsworth, Yacoby, Zibrov, Lukin, Science 326, 267 (2009).

Measure Single Nuclear Spin – the Idea

Nuclear Spin: 

Sensor Spin: 

Suppose:

1. *Initialize sensor spin*
2. *Perform CNOT gate*
3. *Optical readout of sensor spin*
4. **No flip of nuclear spin**

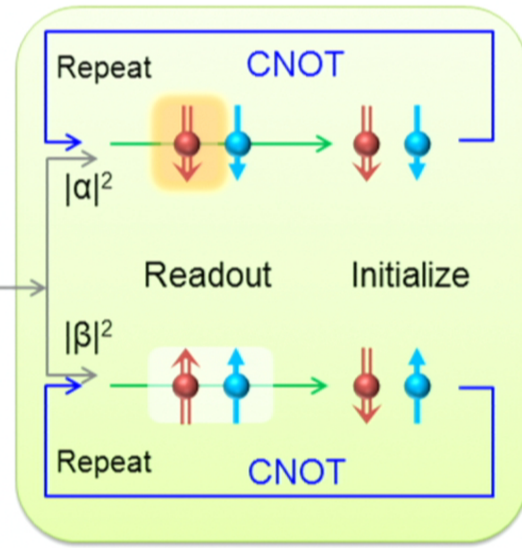

Sensor spin $|0\rangle_e$

Nuclear spin $\alpha|\downarrow\rangle_n + \beta|\uparrow\rangle_n$

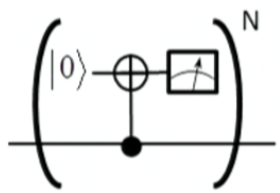

Quantum Non-Demolition (QND)

- Preserve I_z operator.

L.J., Hodges, Maze, Maurer, Taylor, Cory, Hemmer, Walsworth, Yacoby, Zibrov, Lukin, Science 326, 267 (2009).

Diamond Impurities for Spin Sensors

A diamond crystal
(transparent, strong bond, ^{12}C)

Diamond Impurities for Spin Sensors

A diamond crystal
(transparent, strong bond, ^{12}C)

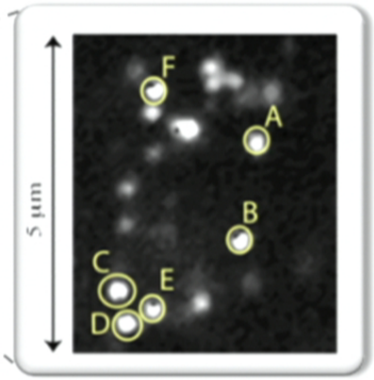

Image of impurity color centers
(NV- centers)

Diamond Impurities for Spin Sensors

A diamond crystal
(transparent, strong bond, ^{12}C)

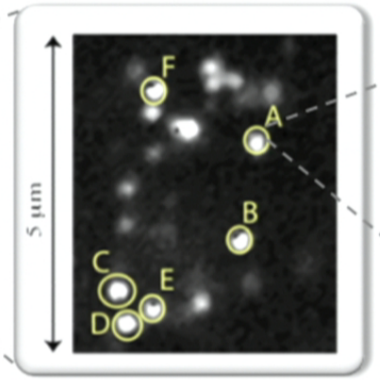

Image of impurity color centers
(NV- centers)

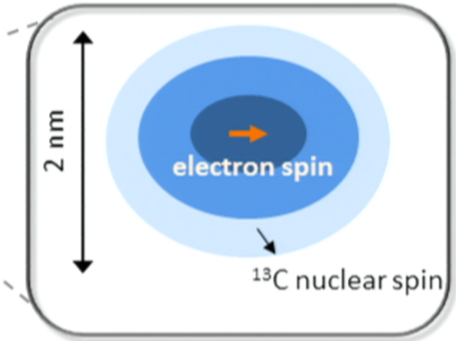

Local spin system
of a single impurity center

Nitrogen-Vacancy (NV-) Impurity:
-- Trapped ion in diamond lattice

✓Stable impurity in diamond

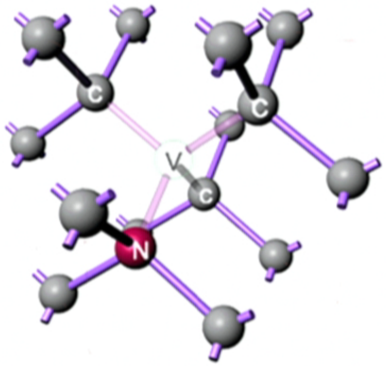

Nitrogen-Vacancy (NV-) Impurity:
-- Trapped ion in diamond lattice

✓Stable impurity in diamond

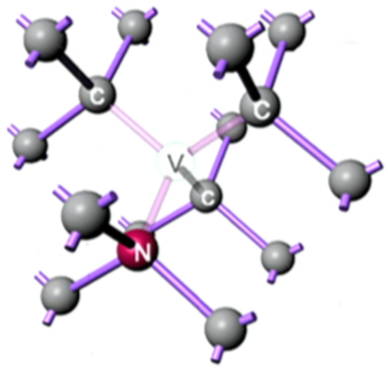

✓Optical properties
- Sharp zero-phonon emission line @ 637 nm
- Can be excited either by 637 nm or 532 nm

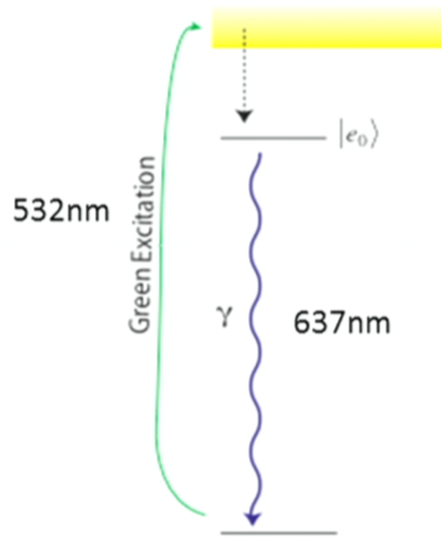

Nitrogen-Vacancy (NV-) Impurity:

-- Trapped ion in diamond lattice

✓Stable impurity in diamond

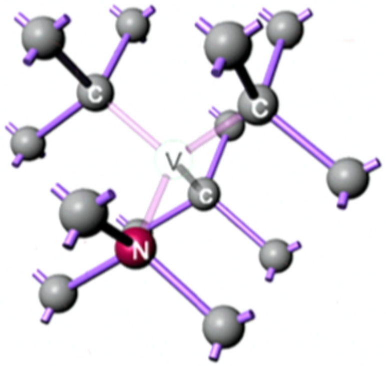

✓Optical properties

- Sharp zero-phonon emission line @ 637 nm
- Can be excited either by 637 nm or 532 nm

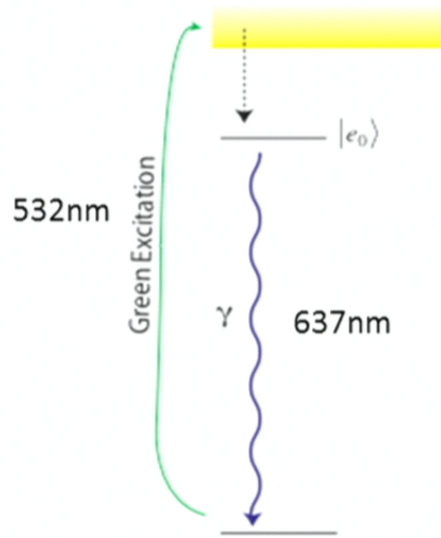

Nitrogen-Vacancy (NV-) Impurity:
-- Trapped ion in diamond lattice

✓Stable impurity in diamond

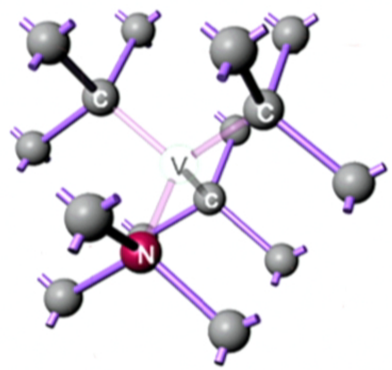

✓Optical properties
- Sharp zero-phonon emission line @ 637 nm
- Can be excited either by 637 nm or 532 nm

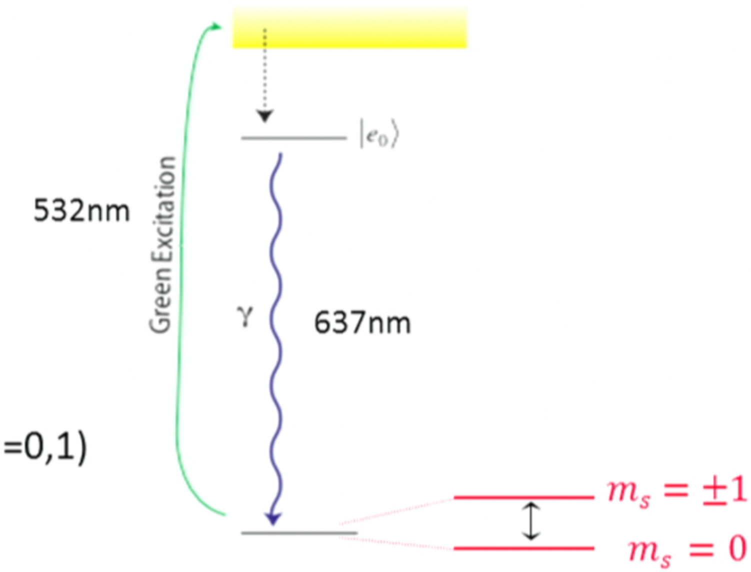

✓Ground state properties
- Non-zero electronic spin (S=1, $|m_s|$=0,1)
- Microwave transition:
  zero-field splitting Δ=2.88 GHz

Control of NV Impurity Electron Spin

Use light to isolate, polarize, readout electron spin qubit @ RT

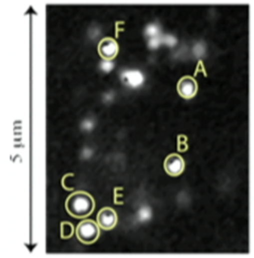

Childress, et al., Science (2006);
Balasubramanian, et al., Nature Mat (2009)

Control of NV Impurity Electron Spin

Use light to isolate, polarize, readout electron spin qubit @ RT

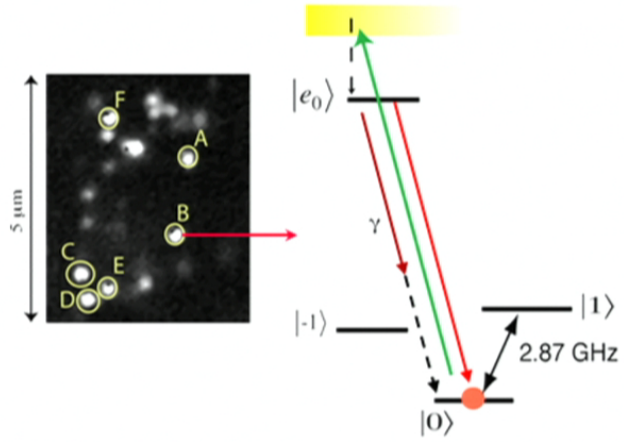

Childress, et al., Science (2006);
Balasubramanian, et al., Nature Mat (2009)

Control of NV Impurity Electron Spin

Use light to isolate, polarize, readout electron spin qubit @ RT

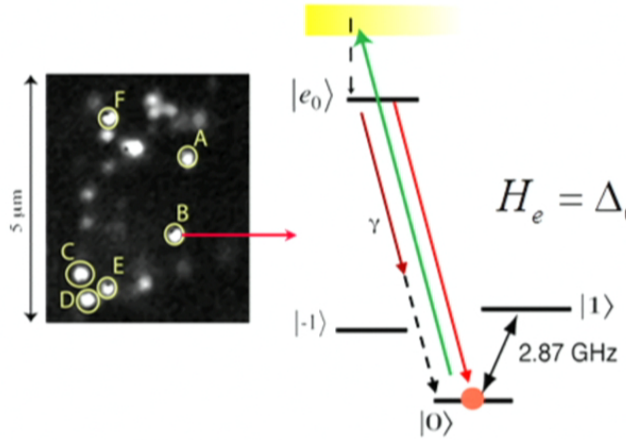

$$H_e = \Delta_0 \hat{S}_z^2 + \mu_e B_z \hat{S}_z$$

Childress, et al., Science (2006);
Balasubramanian, et al., Nature Mat (2009)

Control of NV Impurity Electron Spin

Use light to isolate, polarize, readout electron spin qubit @ RT

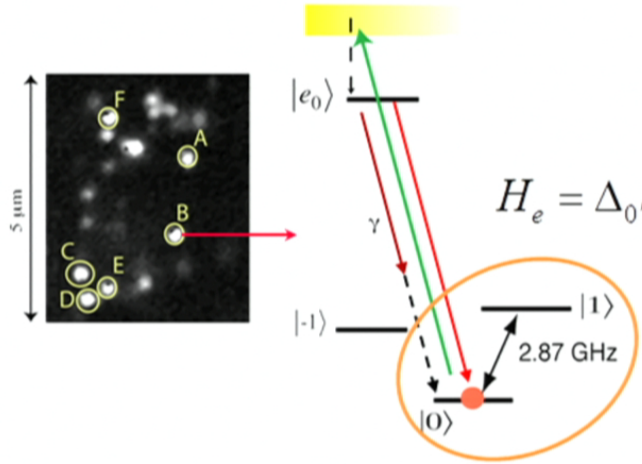

$$H_e = \Delta_0 \hat{S}_z^2 + \mu_e B_z \hat{S}_z$$

Electron T_1

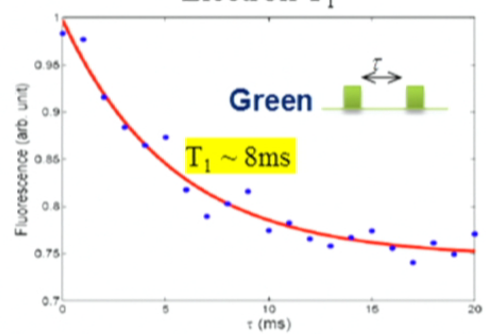

Electron Rabi Oscillation

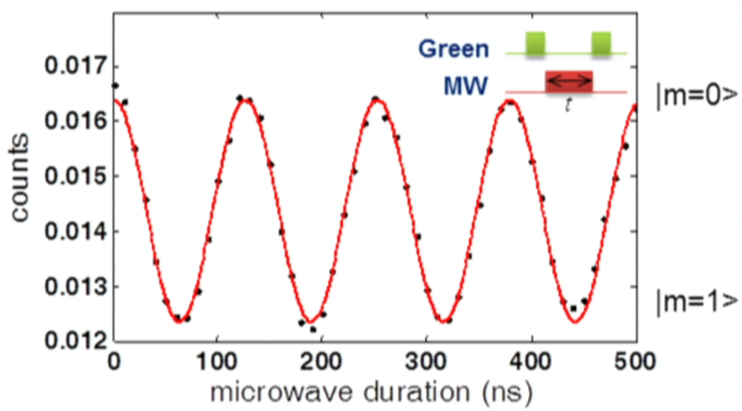

Childress, et al., Science (2006);
Balasubramanian, et al., Nature Mat (2009)

Control of NV Impurity Electron Spin

Use light to isolate, polarize, readout electron spin qubit @ RT

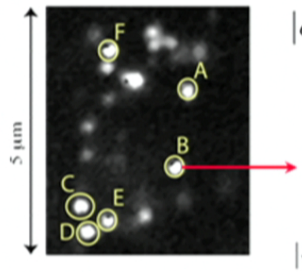

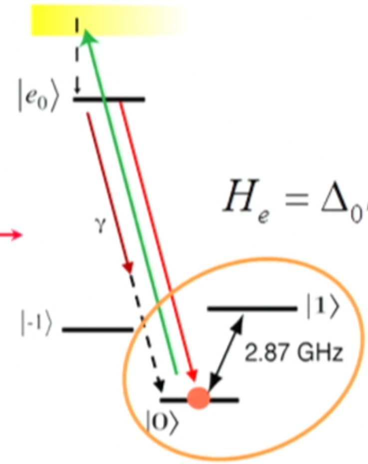

$$H_e = \Delta_0 \hat{S}_z^2 + \mu_e B_z \hat{S}_z$$

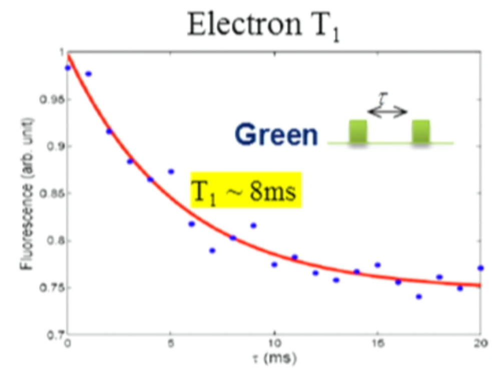

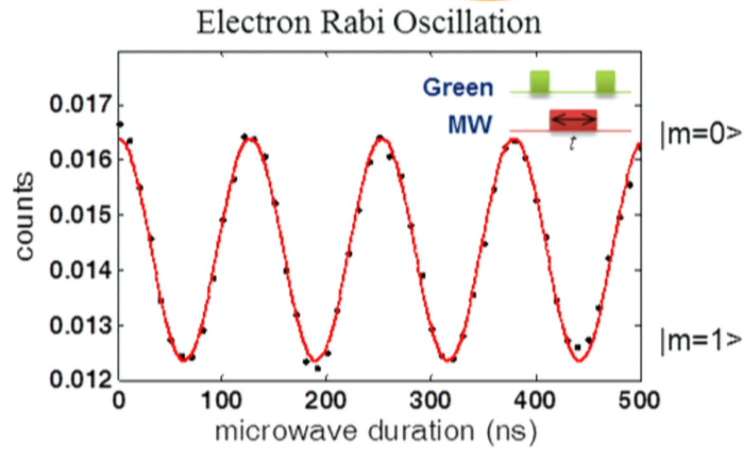

Childress, et al., Science (2006);
Balasubramanian, et al., Nature Mat (2009)

Control of NV Impurity Electron Spin

Use light to isolate, polarize, readout electron spin qubit @ RT

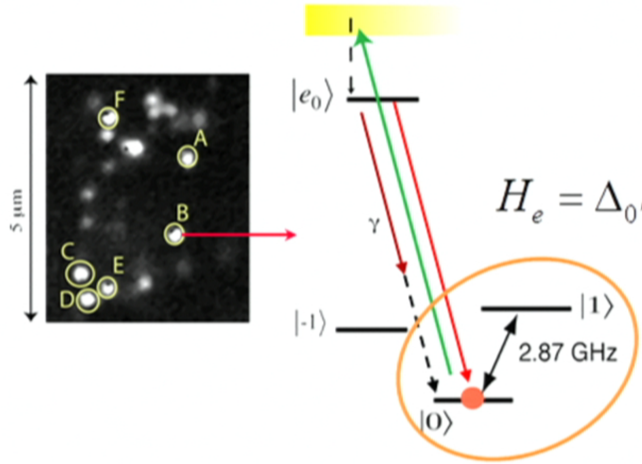

$$H_e = \Delta_0 \hat{S}_z^2 + \mu_e B_z \hat{S}_z$$

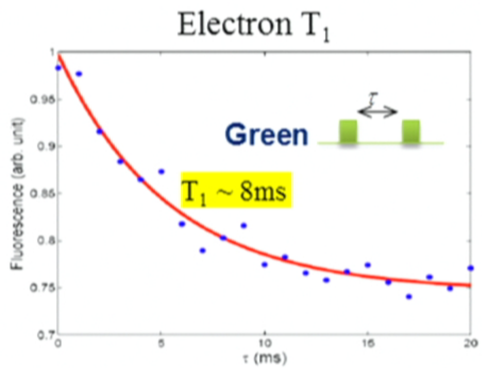

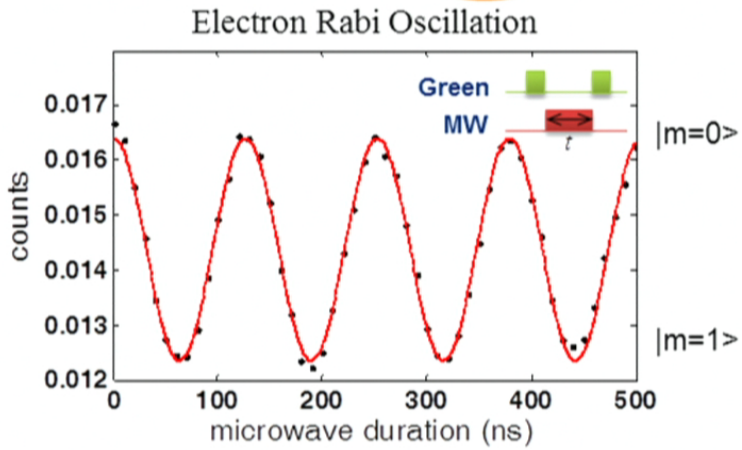

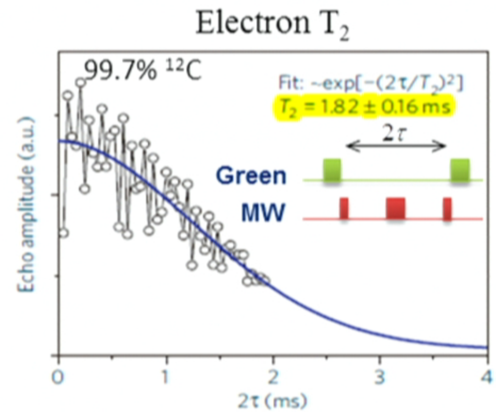

Childress, et al., Science (2006);
Balasubramanian, et al., Nature Mat (2009)

Control of NV Impurity Electron Spin

Use light to isolate, polarize, readout electron spin qubit @ RT

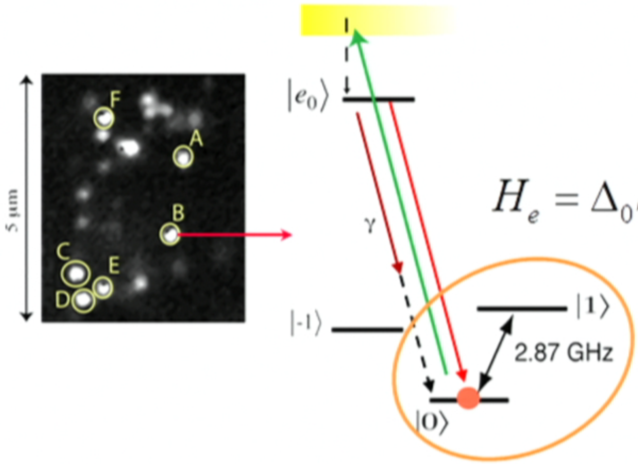

$$H_e = \Delta_0 \hat{S}_z^2 + \mu_e B_z \hat{S}_z$$

Electron T_1

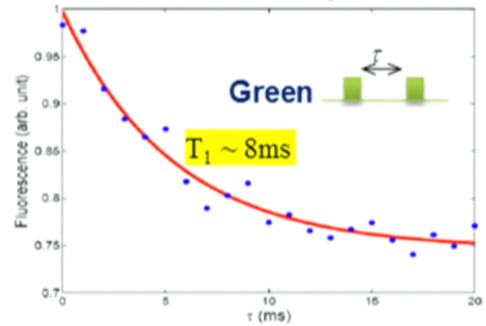

Electron Rabi Oscillation

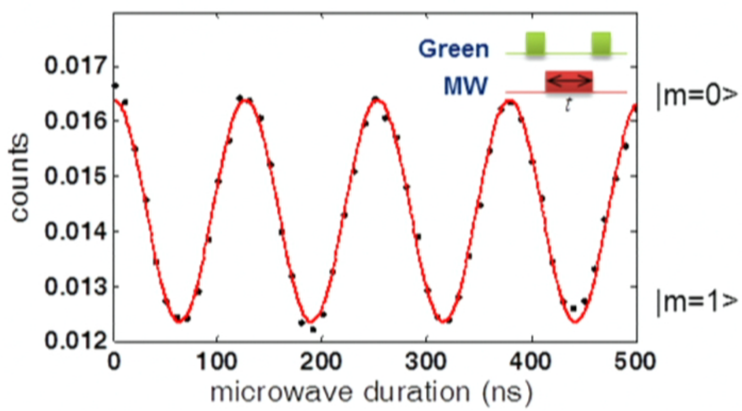

Electron T_2

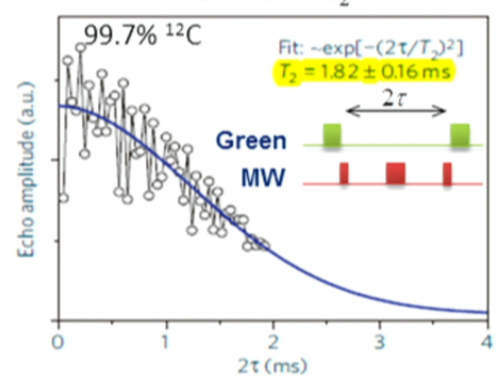

Childress, et al., Science (2006);
Balasubramanian, et al., Nature Mat (2009)

Isotopically Pure Diamond (with 99.99% ^{12}C)

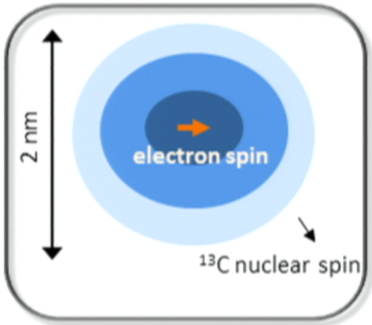

Diamond with $<10^{-4}$ isotope ^{13}C

Isotopically Pure Diamond (with 99.99% ^{12}C)

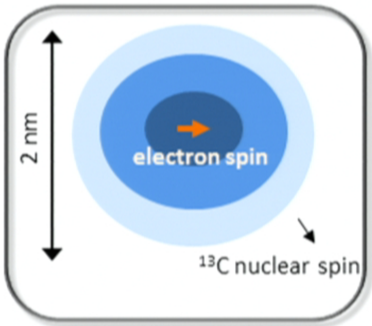

Diamond with <10^{-4} isotope ^{13}C

$$H_{nuc} = AS_zI_z + \omega I_z$$

- Zeeman dominated regime ($r \approx$ 1.5nm)
  $\omega = \mu_I B_z \sim 0.5\text{MHz} \gg A = \frac{\mu_e \mu_I}{r^3} \sim 2.7kHz$

Isotopically Pure Diamond (with 99.99% ^{12}C)

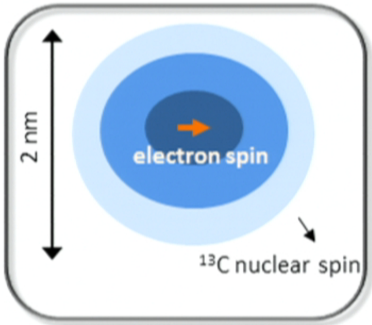

Diamond with <10⁻⁴ isotope ¹³C

$$H_{nuc} = A S_z I_z + \omega I_z$$

- Zeeman dominated regime ($r \approx 1.5$nm)
  $\omega = \mu_I B_z \sim 0.5\text{MHz} \gg A = \frac{\mu_e \mu_I}{r^3} \sim 2.7kHz$

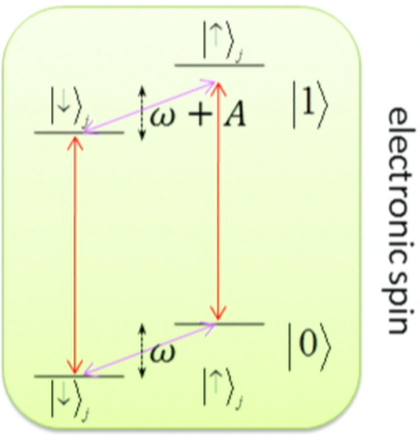

Nuclear spin *I=1/2*

Isotopically Pure Diamond (with 99.99% ^{12}C)

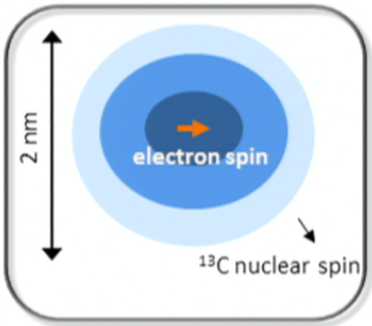

Diamond with $<10^{-4}$ isotope ^{13}C

$$H_{nuc} = A S_z I_z + \omega I_z$$

- Zeeman dominated regime ($r \approx 1.5$nm)
  $\omega = \mu_I B_z \sim 0.5\text{MHz} \gg A = \frac{\mu_e \mu_I}{r^3} \sim 2.7kHz$

- Implement **$C_n NOT_e$ gate**

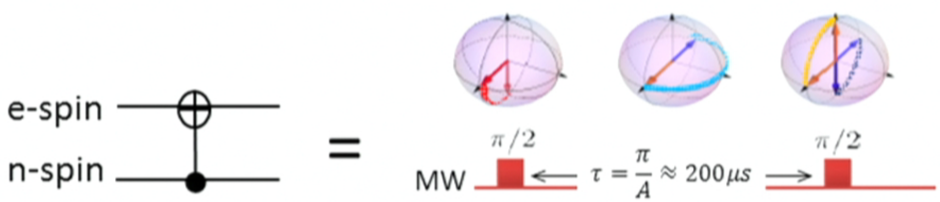

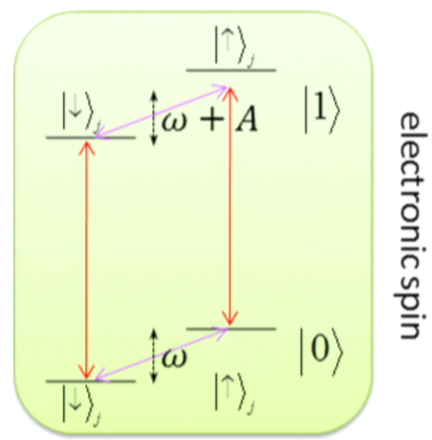

Nuclear spin $I=1/2$

Isotopically Pure Diamond (with 99.99% ^{12}C)

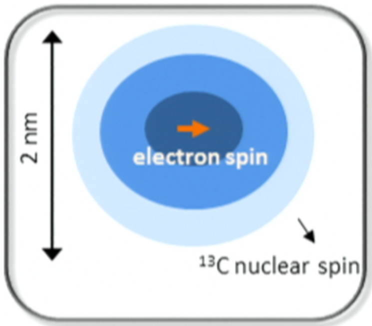

Diamond with <10^{-4} isotope ^{13}C

$$H_{nuc} = A S_z I_z + \omega I_z$$

- Zeeman dominated regime ($r \approx 1.5$nm)
  $\omega = \mu_I B_z \sim 0.5\text{MHz} \gg A = \frac{\mu_e \mu_I}{r^3} \sim 2.7kHz$

- Implement $\mathbf{C_n NOT_e}$ **gate**

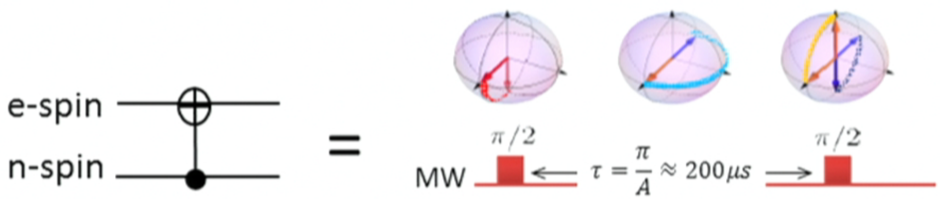

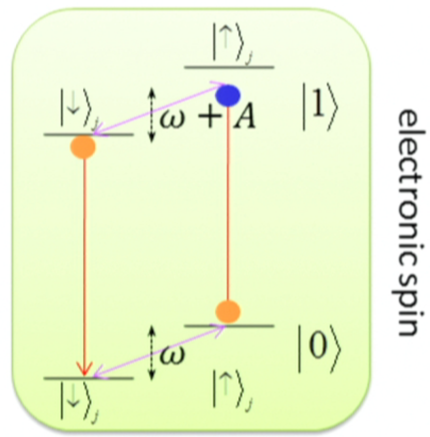

Nuclear spin *I=1/2*

Isotopically Pure Diamond (with 99.99% ^{12}C)

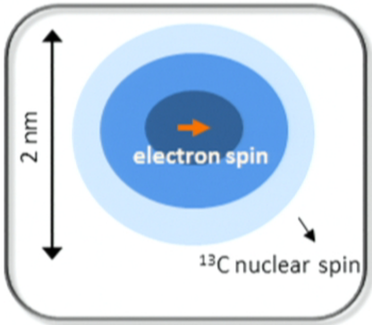

Diamond with <10^{-4} isotope ^{13}C

$$H_{nuc} = AS_zI_z + \omega I_z$$

- Zeeman dominated regime ($r \approx$ 1.5nm) $\omega = \mu_I B_z \sim 0.5\text{MHz} \gg A = \frac{\mu_e \mu_I}{r^3} \sim 2.7kHz$

- Implement **$C_n NOT_e$ gate**

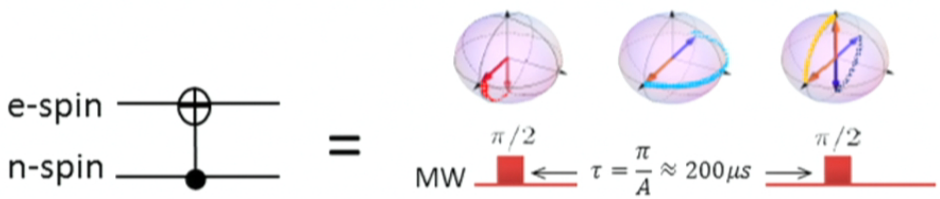

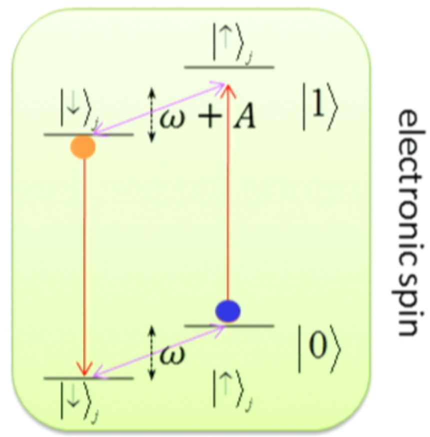

Nuclear spin *I=1/2*

Quantum Jumps of Nuclear Spin

- Approach: Repetitively use C_nNOT_e gate to readout nuclear spin. (I_z is QND observable)

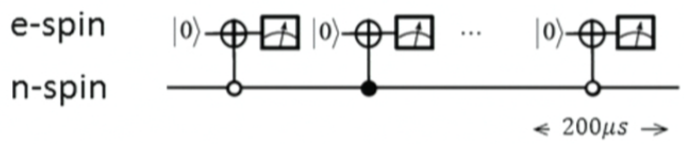

Quantum Jumps of Nuclear Spin

- Approach: Repetitively use C_nNOT_e gate to readout nuclear spin. (I_z is QND observable)

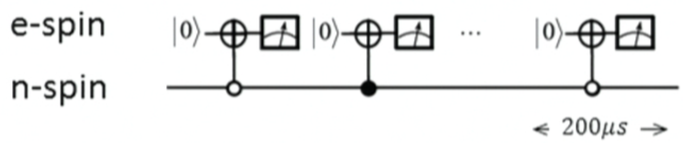

- Readout provides single shot measurement of I_z. ($N = 20{,}000$)

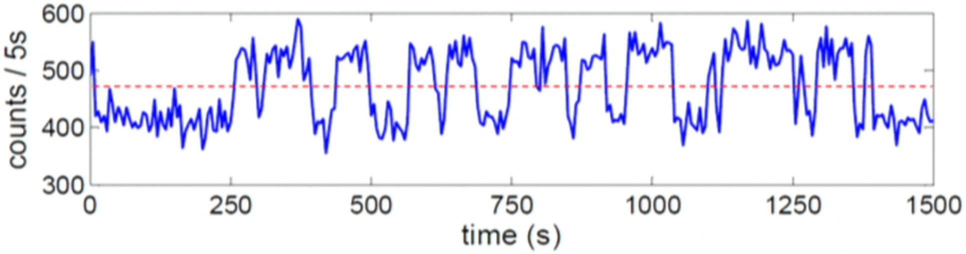

Quantum Jumps of Nuclear Spin

- Approach: Repetitively use C_nNOT_e gate to readout nuclear spin. (I_z is QND observable)

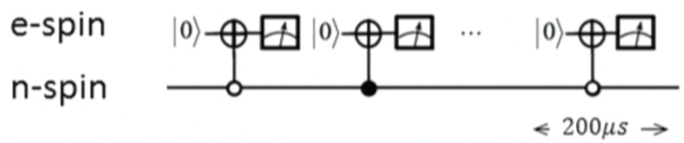

- Readout provides single shot measurement of I_z. ($N = 20{,}000$)

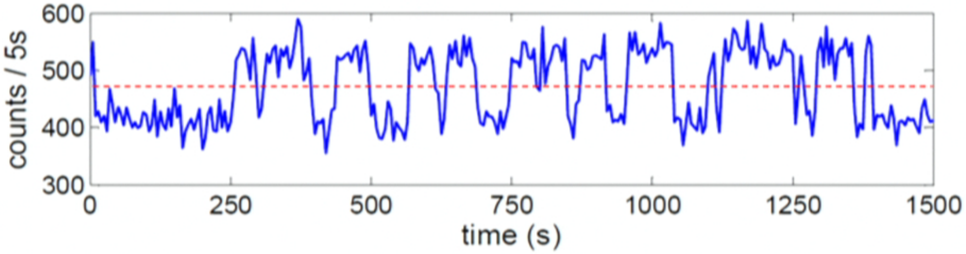

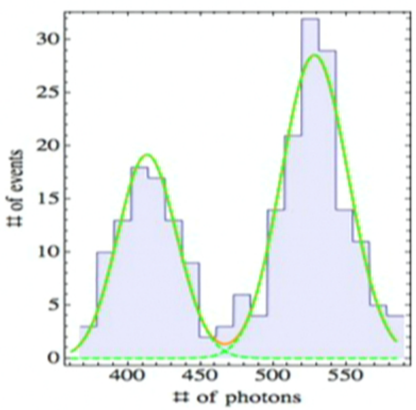

Quantum Jumps of Nuclear Spin

- Approach: Repetitively use C_nNOT_e gate to readout nuclear spin. (I_z is QND observable)

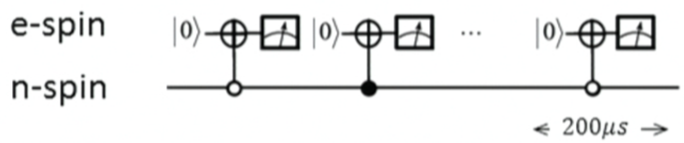

- Readout provides single shot measurement of I_z. ($N = 20{,}000$)

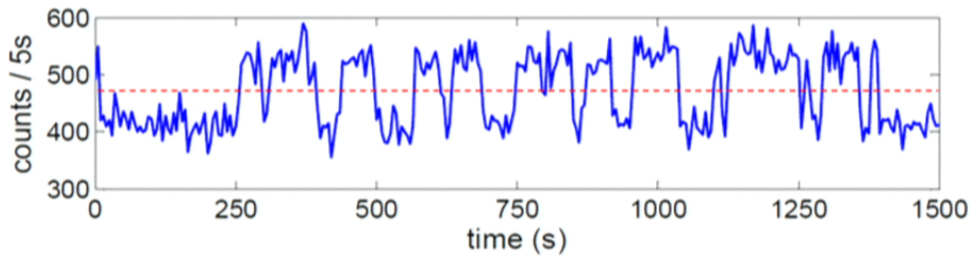

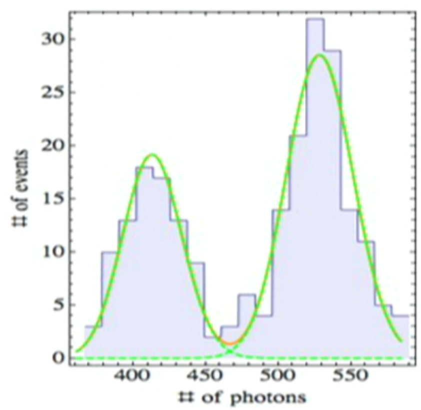

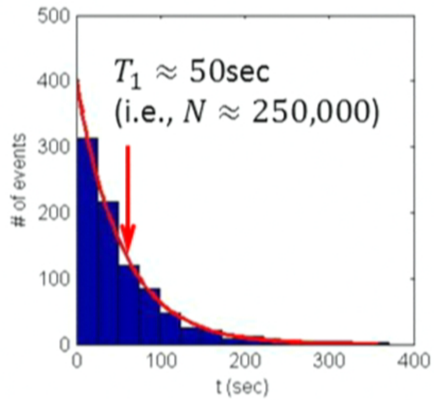

Fidelity of Repetitive QND Measurement

- Initialization with post-selection

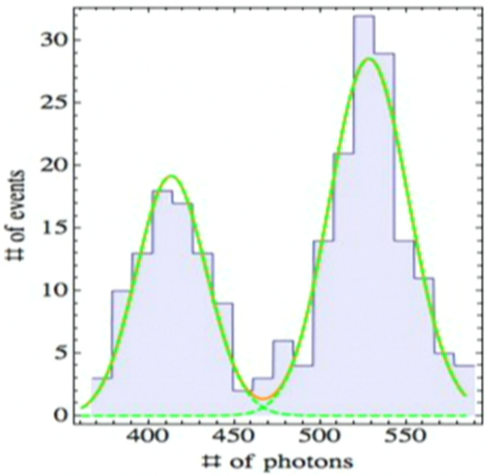

Fidelity of Repetitive QND Measurement

- Initialization with post-selection

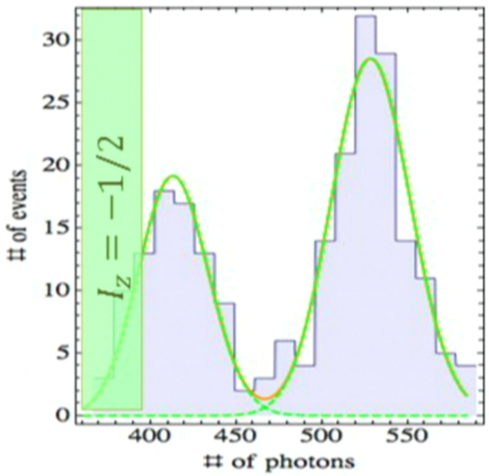

Fidelity of Repetitive QND Measurement

- Initialization with post-selection

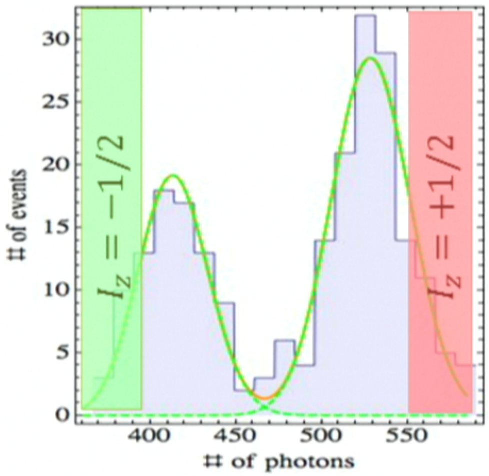

Fidelity of Repetitive QND Measurement

- Initialization with post-selection

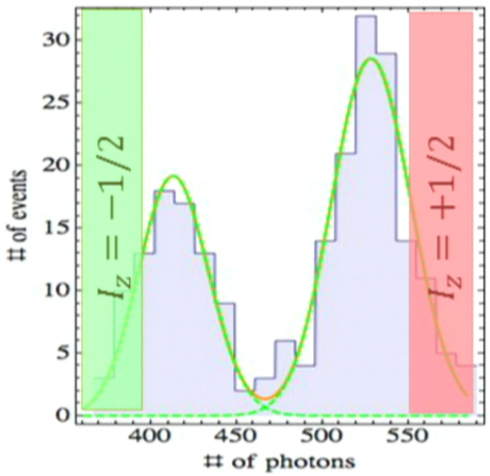

- Repetitive QND measurement of nucleus with $N = 20000$ (i.e., $N\tau \approx 4\text{sec}$)

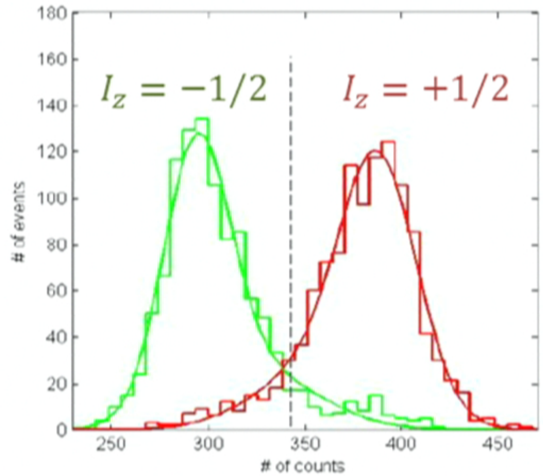

Fidelity of Repetitive QND Measurement

- Initialization with post-selection

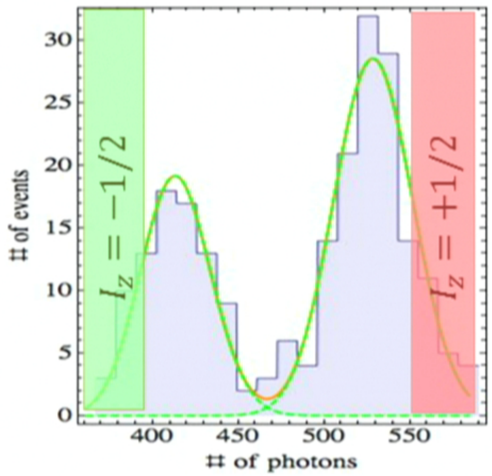

- Repetitive QND measurement of nucleus with $N = 20000$ (i.e., $N\tau \approx 4$sec)

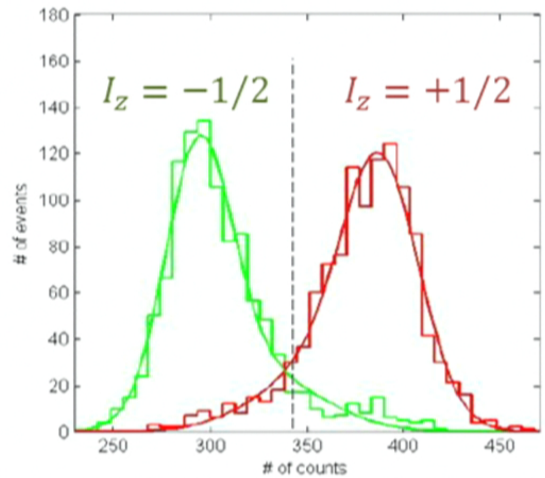

Good Readout fidelity ≈ **92%**

- Imperfections
  -- Non-ideal QND operation with $\epsilon \approx 4 \times 10^{-6}$ bit-flip for each readout.

- Potential improvement using *generalized* maximum likelihood estimate (MLE).

Coherence of Nuclear Spin Memory

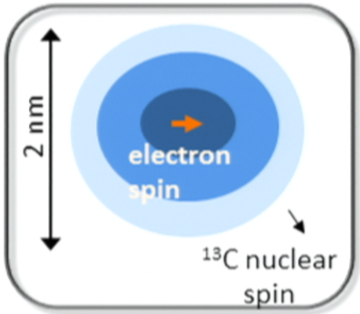

- Three Major Decoherence Mechanisms
  1. Dephasing from the electron spin ($T_{1e} \approx 8ms$)
  2. Dephasing due to residual magnetic field (δB_z)
  3. Dipole coupling with other nuclear spins ($r \sim 2nm, \frac{\mu^2}{r^3} \sim 1Hz$)
- Decoupling Techniques to Suppress Decoherence
  1. Green laser (suppress electron-spin-induced dephasing)
  2. Spin echo (suppress δB_z)
  3. MREV-8 Decoupling (suppress dipole coupling)

Duer, M. J., "Solid-state NMR spectroscopy: principles and applications" page 87.

Fidelity of Repetitive QND Measurement

- Initialization with post-selection

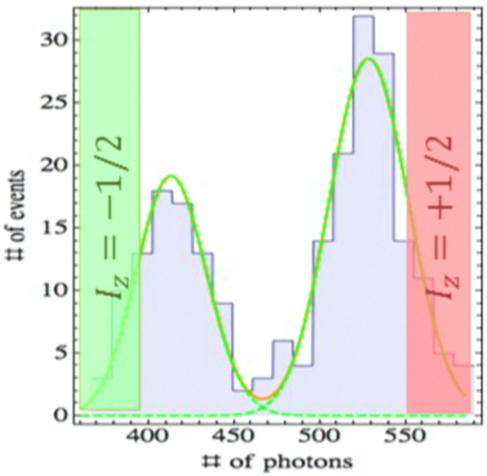

- Repetitive QND measurement of nucleus with $N = 20000$ (i.e., $N\tau \approx 4$sec)

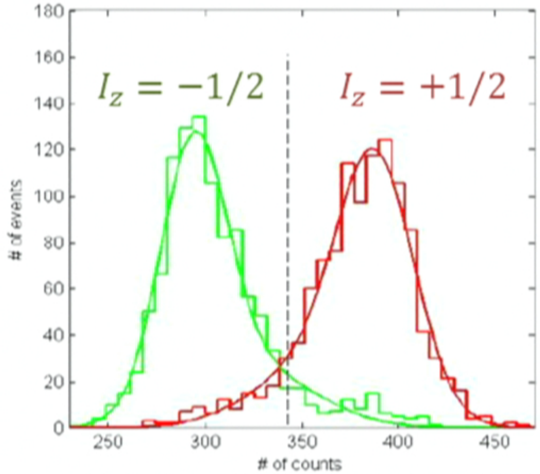

Good Readout fidelity ≈ **92%**

- Imperfections
  -- Non-ideal QND operation with $\epsilon \approx 4 \times 10^{-6}$ bit-flip for each readout.

- Potential improvement using *generalized* maximum likelihood estimate (MLE).

Coherence of Nuclear Spin Memory

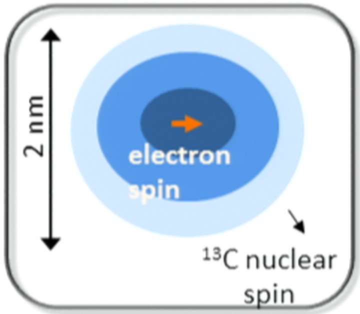

- Three Major Decoherence Mechanisms
  1. Dephasing from the electron spin ($T_{1e} \approx 8ms$)
  2. Dephasing due to residual magnetic field (δB_z)
  3. Dipole coupling with other nuclear spins ($r \sim 2nm, \frac{\mu^2}{r^3} \sim 1Hz$)
- Decoupling Techniques to Suppress Decoherence
  1. Green laser (suppress electron-spin-induced dephasing)
  2. Spin echo (suppress δB_z)
  3. MREV-8 Decoupling (suppress dipole coupling)

Duer, M. J., "Solid-state NMR spectroscopy: principles and applications" page 87.

Coherence of Nuclear Spin Memory

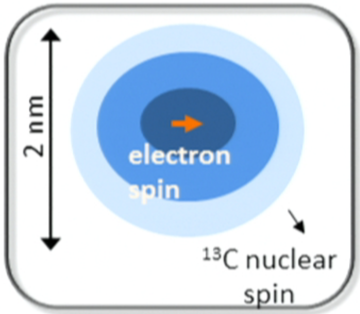

- Three Major Decoherence Mechanisms
  1. Dephasing from the electron spin ($T_{1e} \approx 8ms$)
  2. Dephasing due to residual magnetic field (δB_z)
  3. Dipole coupling with other nuclear spins ($r \sim 2nm, \frac{\mu^2}{r^3} \sim 1Hz$)
- Decoupling Techniques to Suppress Decoherence
  1. Green laser (suppress electron-spin-induced dephasing)
  2. Spin echo (suppress δB_z)
  3. MREV-8 Decoupling (suppress dipole coupling)

Duer, M. J., "Solid-state NMR spectroscopy: principles and applications" page 87.

Coherence of Nuclear Spin Memory (Ramsey Exp.)

Decoupling Techniques to Suppress Decoherence

1. Green laser (electron-spin-induced dephasing)
2. Spin echo (suppress δB_z)
3. MREV-8 Decoupling (suppress dipole coupling)

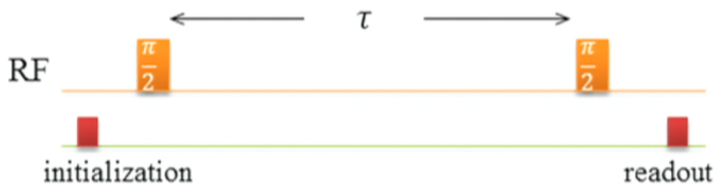

Maurer, Kusko, Latta, L J, et al. (to be submitted)

Coherence of Nuclear Spin Memory (Ramsey Exp.)

Decoupling Techniques to Suppress Decoherence

1. Green laser (electron-spin-induced dephasing)
2. Spin echo (suppress δB_z)
3. MREV-8 Decoupling (suppress dipole coupling)

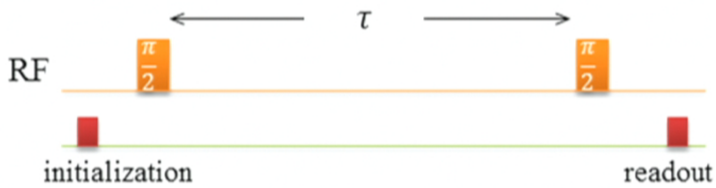

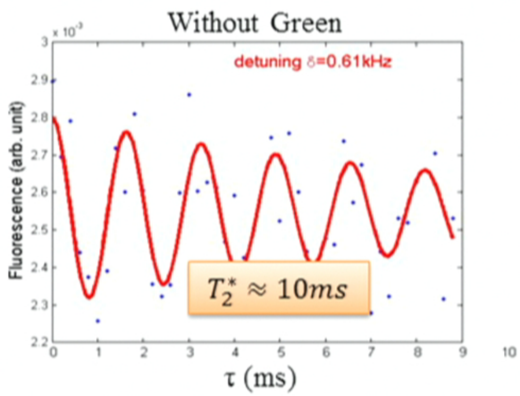

Maurer, Kusko, Latta, L J, et al. (to be submitted)

Coherence of Nuclear Spin Memory (Ramsey Exp.)

Decoupling Techniques to Suppress Decoherence

1. Green laser (electron-spin-induced dephasing)
2. Spin echo (suppress δB_z)
3. MREV-8 Decoupling (suppress dipole coupling)

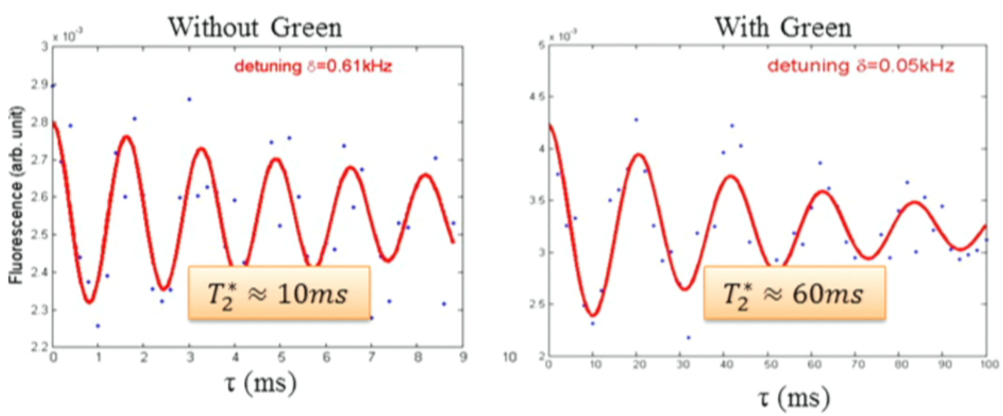

Maurer, Kusko, Latta, L J, et al. (to be submitted)

Coherence of Nuclear Spin Memory (Ramsey Exp.)

Decoupling Techniques to Suppress Decoherence

1. Green laser (electron-spin-induced dephasing)
2. Spin echo (suppress δB_z)
3. MREV-8 Decoupling (suppress dipole coupling)

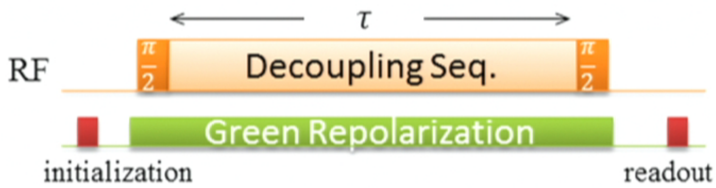

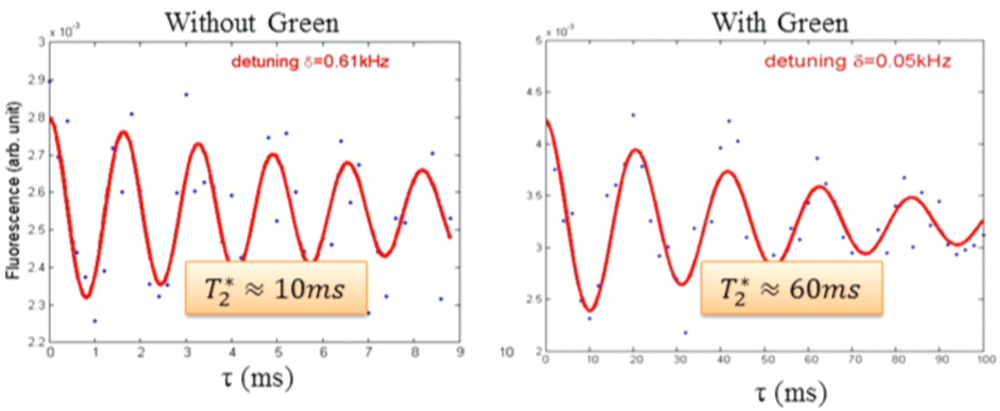

Maurer, Kusko, Latta, L J, et al. (to be submitted)

Coherence of Nuclear Spin Memory (Ramsey Exp.)

Decoupling Techniques to Suppress Decoherence

1. Green laser (electron-spin-induced dephasing)
2. Spin echo (suppress δB_z)
3. MREV-8 Decoupling (suppress dipole coupling)

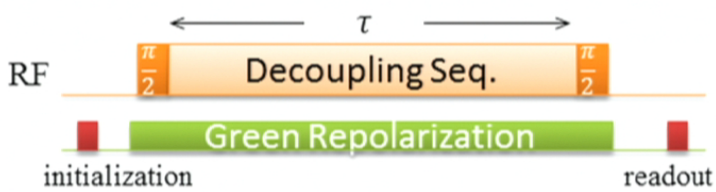

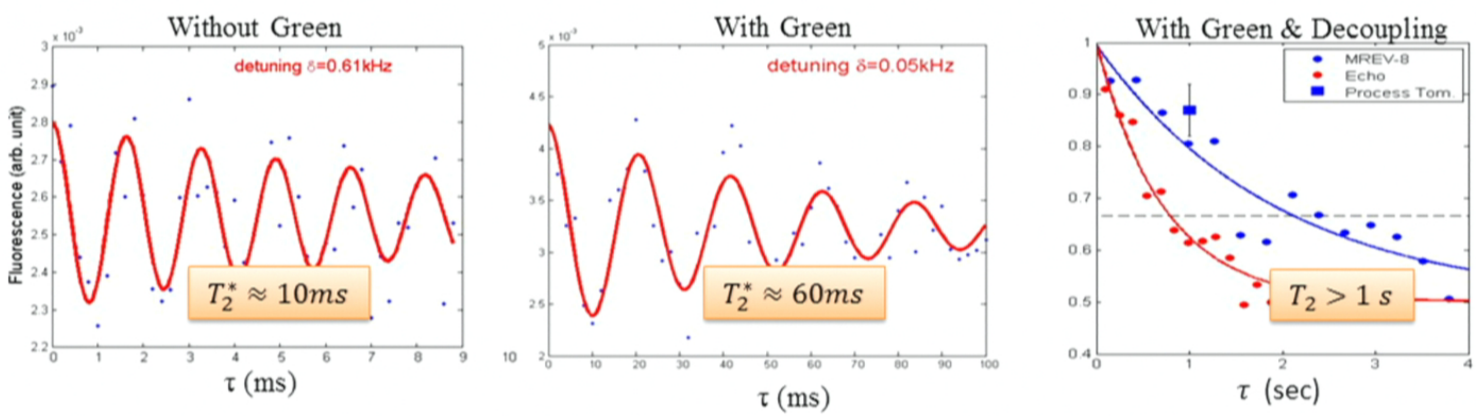

Maurer, Kusko, Latta, L J, et al. (to be submitted)

Coherence of Nuclear Spin Memory (Ramsey Exp.)

Decoupling Techniques to Suppress Decoherence

1. Green laser (electron-spin-induced dephasing)
2. Spin echo (suppress δB_z)
3. MREV-8 Decoupling (suppress dipole coupling)

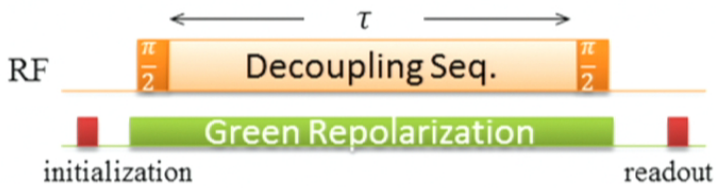

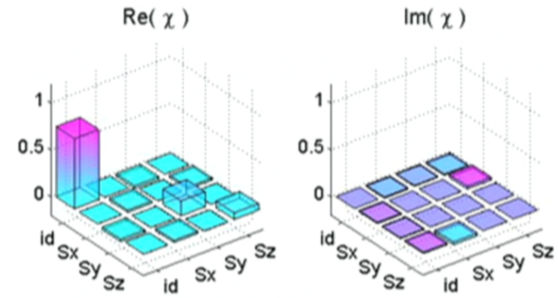

Average fidelity $F = (87 \pm 5)\%$ for 1 second storage time.

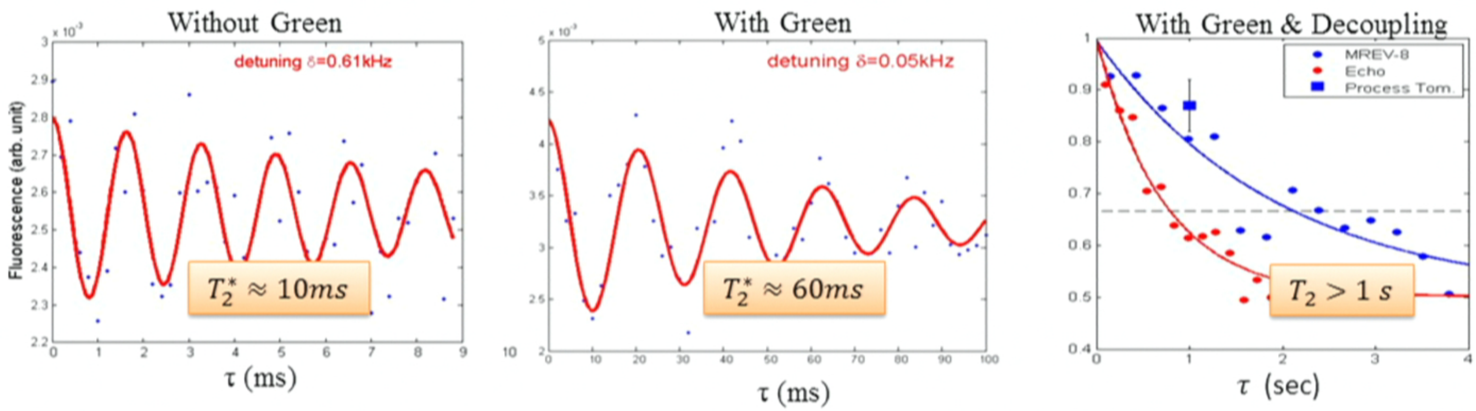

Maurer, Kusko, Latta, L J, et al. (to be submitted)

Laser Power Dependence

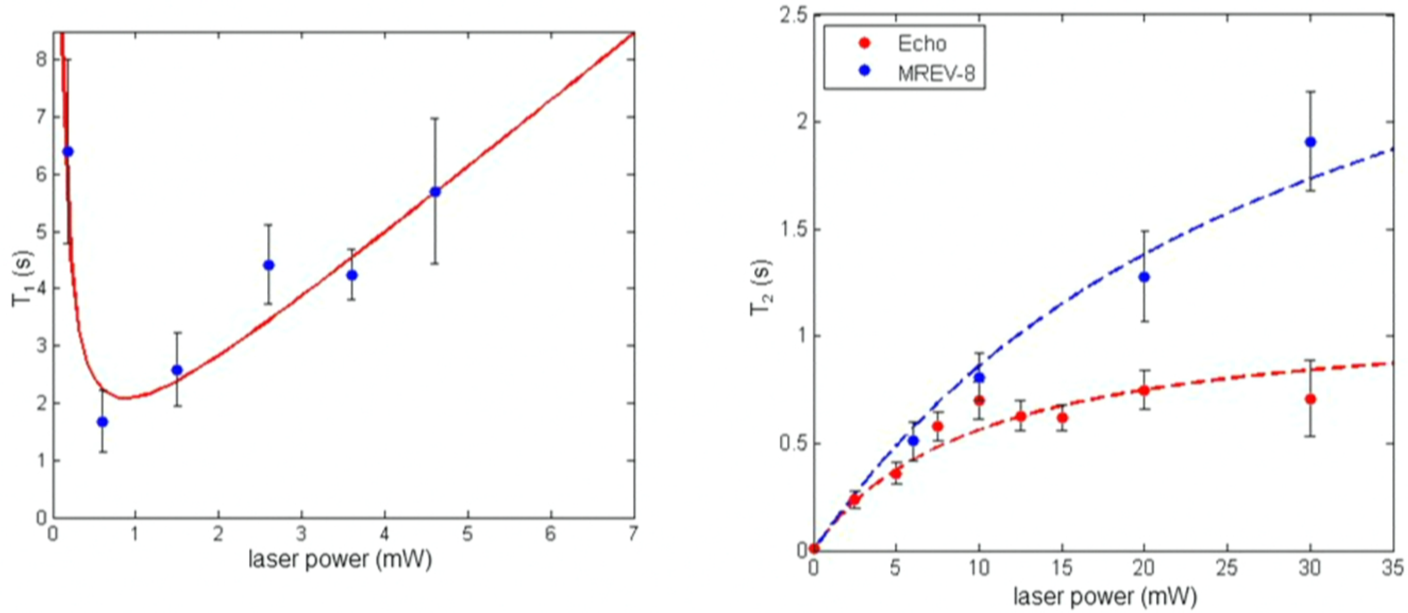

For strong optical illumination, both $T_{1,n}$ and $T_{2,n}$ increase **linearly** with laser power.

Maurer, Kusko, Latta, L J, et al. (to be submitted)

Laser Power Dependence

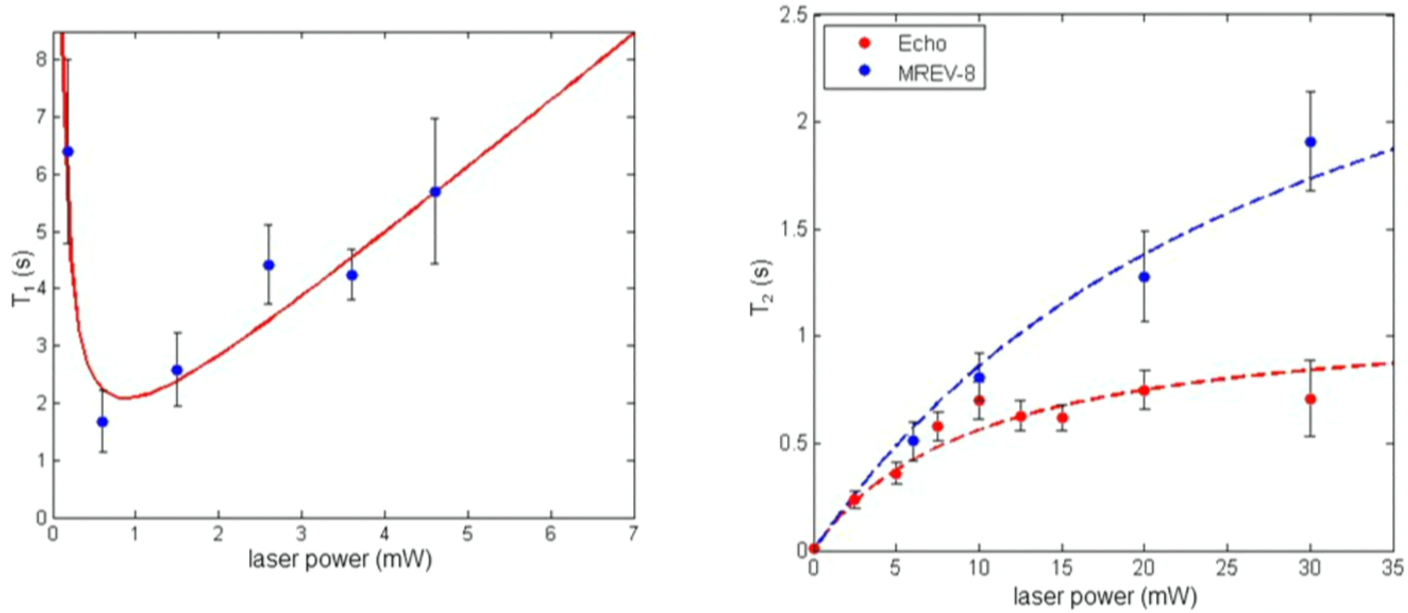

For strong optical illumination, both $T_{1,n}$ and $T_{2,n}$ increase **linearly** with laser power.

Maurer, Kusko, Latta, L J, et al. (to be submitted)

Laser Power Dependence

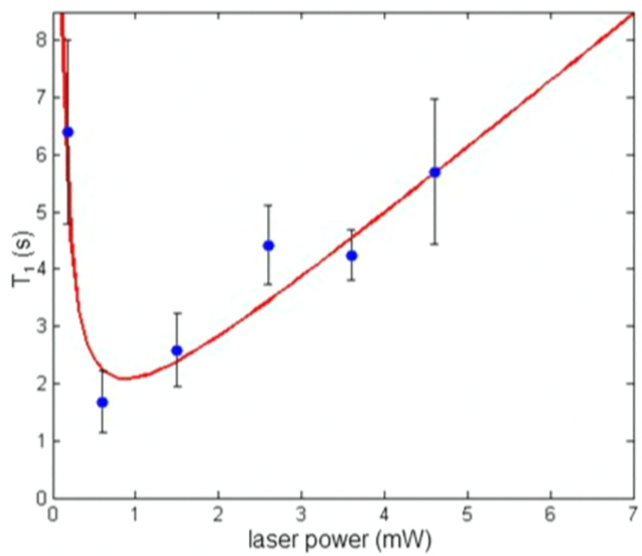

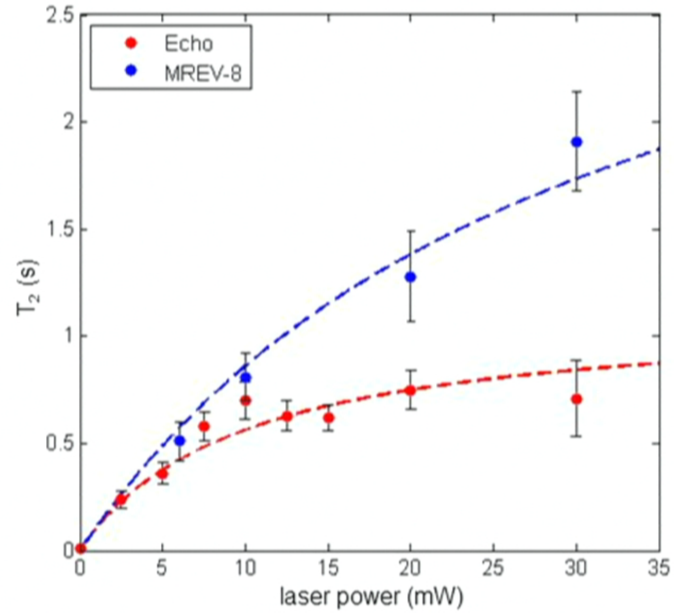

For strong optical illumination, both $T_{1,n}$ and $T_{2,n}$ increase **linearly** with laser power.

Maurer, Kusko, Latta, L J, et al. (to be submitted)

Laser Power Dependence

-- Motional Averaging

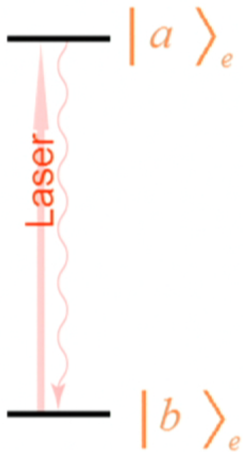

L.J., Dutt, Childress, *et al.*, PRL 100, 073001 (2008)

Laser Power Dependence
-- Motional Averaging

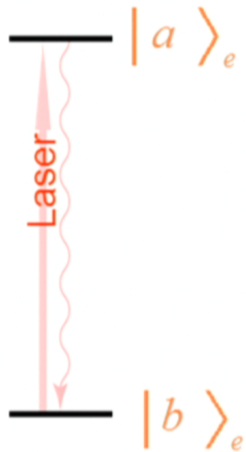

L.J., Dutt, Childress, *et al.*, PRL 100, 073001 (2008)

Laser Power Dependence

-- Motional Averaging

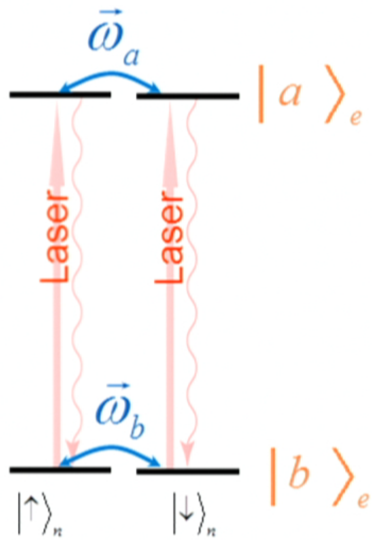

L.J., Dutt, Childress, *et al.*, PRL 100, 073001 (2008)

Laser Power Dependence

-- Motional Averaging

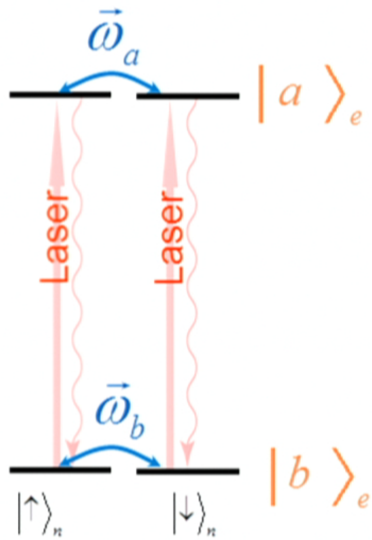

Two-State Spin-Fluctuator Model

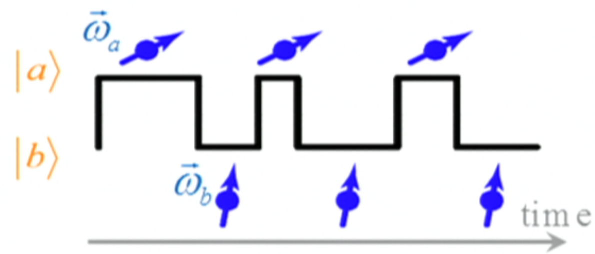

1. Incoherent stochastic transition between |a> & |b>, with rate R.
2. Coherent evolution of n-spin.

L.J., Dutt, Childress, *et al.*, PRL 100, 073001 (2008)

Laser Power Dependence

-- Motional Averaging

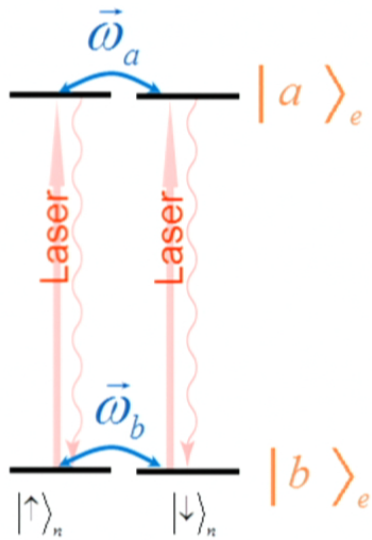

Two-State Spin-Fluctuator Model

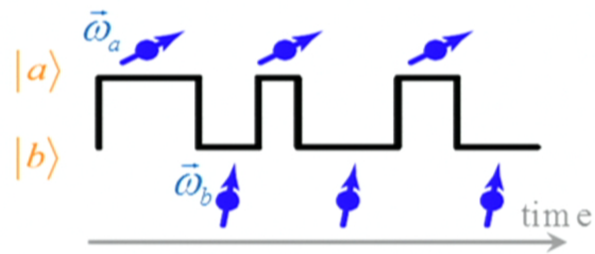

1. Incoherent stochastic transition between |a> & |b>, with rate R.
2. Coherent evolution of n-spin.

Solve Master Equations:

$$\Gamma \approx \frac{\Delta\omega^2}{R} \qquad \text{for } |\Delta\omega| << R$$

L.J., Dutt, Childress, *et al.*, PRL 100, 073001 (2008)

Laser Power Dependence
-- Motional Averaging

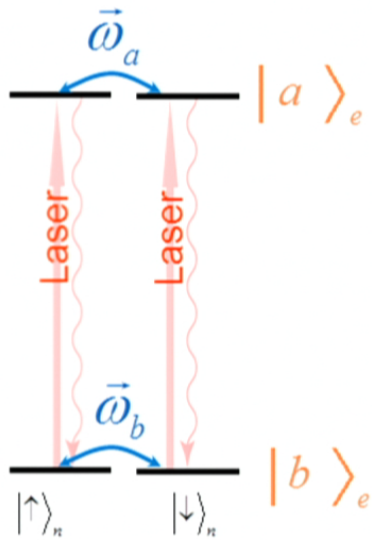

Two-State Spin-Fluctuator Model

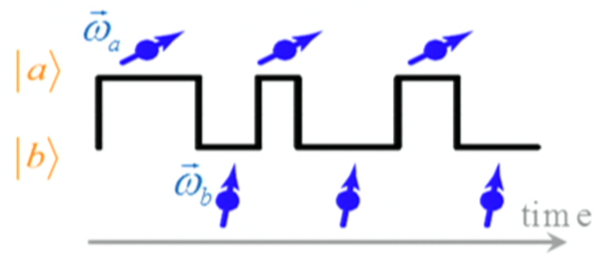

1. Incoherent stochastic transition between |a> & |b>, with rate R.
2. Coherent evolution of n-spin.

Solve Master Equations:

$$\Gamma \approx \frac{\Delta\omega^2}{R} \qquad \text{for } |\Delta\omega| << R$$

The faster the stochastic motion, the better the coherence!

L.J., Dutt, Childress, *et al.*, PRL 100, 073001 (2008)

Application: Quantum Money @ RT

- Encode secure information in array of solid-state qubits
- Basic Idea
  - Initialize a product state of individual qubits in arbitrary basis only known to issuer
- Advantages:
  - Impossible to copy (**no-cloning principle**)
  - Attempt to read the array by third party will leave a trace (chance to crack 2^{-N})
- Requirements
  - Solid state system and room temperature ✔
  - High fidelity readout ✔
  - Long coherence time **(Possible to extend to mins/hours)**

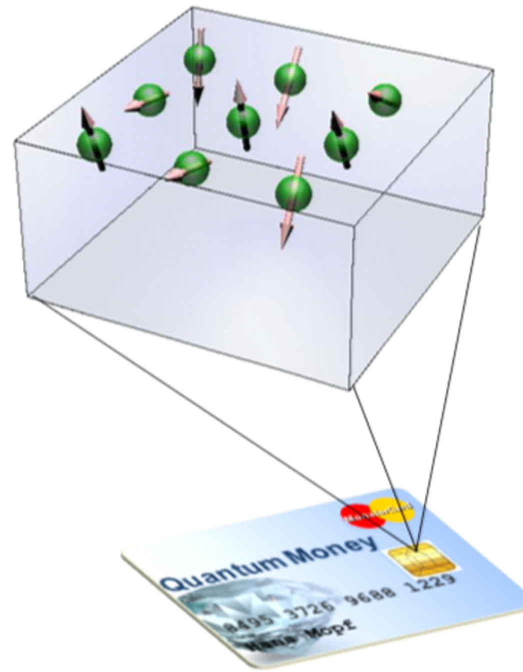

S. Wiesner. Conjugate coding. SIGACT News, 15(1):78–88, 1983.

Application: Quantum Money @ RT

- Encode secure information in array of solid-state qubits
- Basic Idea
    - Initialize a product state of individual qubits in arbitrary basis only known to issuer
- Advantages:
    - Impossible to copy (**no-cloning principle**)
    - Attempt to read the array by third party will leave a trace (chance to crack 2^{-N})
- Requirements
    - Solid state system and room temperature ✓
    - High fidelity readout ✓
    - Long coherence time **(Possible to extend to mins/hours)**

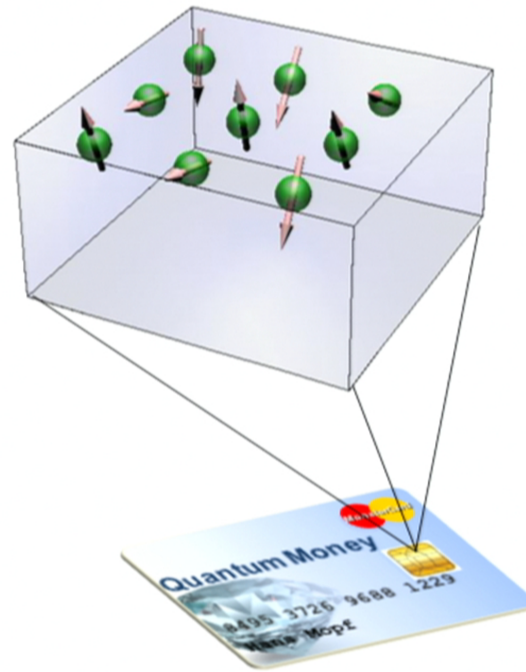

S. Wiesner. Conjugate coding. SIGACT News, 15(1):78–88, 1983.

Question: Quantum Computer @ RT?

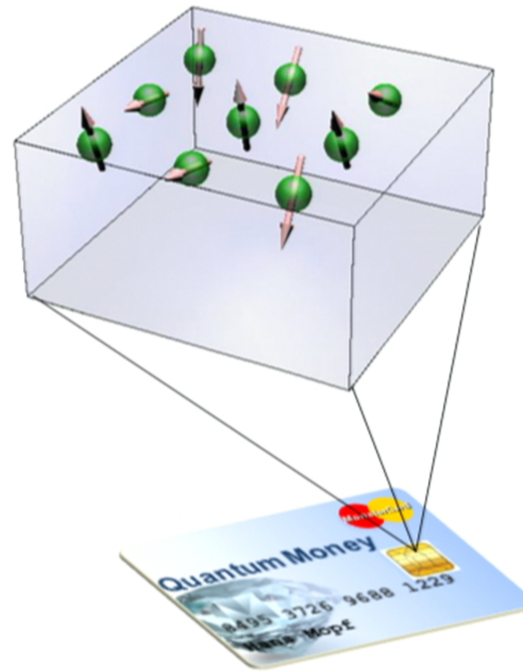

Question: Quantum Computer @ RT?

PRL 106, 040505 (2011) PHYSICAL REVIEW LETTERS week ending 28 JANUARY 2011

Robust Quantum State Transfer in Random Unpolarized Spin Chains

N. Y. Yao,[1] L. Jiang,[2] A. V. Gorshkov,[1,2] Z.-X. Gong,[3] A. Zhai,[4] L.-M. Duan,[3] and M. D. Lukin[1]
[1]*Department of Physics, Harvard University, Cambridge, Massachusetts 02138, USA*
[2]*IQI, California Institute of Technology, Pasadena, California 91125, USA*
[3]*Department of Physics and MCTP, University of Michigan, Ann Arbor, Michigan 48109, USA*
[4]*Department of Mathematics, Harvard University, Cambridge, Massachusetts 02138, USA*
(Received 14 November 2010; published 27 January 2011)

Question: Quantum Computer @ RT?

PRL 106, 040505 (2011) PHYSICAL REVIEW LETTERS week ending 28 JANUARY 2011

Robust Quantum State Transfer in Random Unpolarized Spin Chains

N. Y. Yao,[1] L. Jiang,[2] A. V. Gorshkov,[1,2] Z.-X. Gong,[3] A. Zhai,[4] L.-M. Duan,[3] and M. D. Lukin[1]
[1]*Department of Physics, Harvard University, Cambridge, Massachusetts 02138, USA*
[2]*IQI, California Institute of Technology, Pasadena, California 91125, USA*
[3]*Department of Physics and MCTP, University of Michigan, Ann Arbor, Michigan 48109, USA*
[4]*Department of Mathematics, Harvard University, Cambridge, Massachusetts 02138, USA*
(Received 14 November 2010; published 27 January 2011)

Scalable Architecture for a Room Temperature Solid-State Quantum Information Processor

N. Y. Yao[1†*], L. Jiang[2†], A. V. Gorshkov[1,2†], P. C. Maurer[1], G. Giedke[3], J. I. Cirac[3], M. D. Lukin[1]
[1]*Physics Department, Harvard University, Cambridge, MA 02138*
[2]*Institute for Quantum Information, California Institute of Technology, Pasadena, CA 91125*
[3]*Max-Planck-Institut für Quantenoptik, Hans-Kopfermann-Strasse 1, Garching, D-85748, Germany*
[†]*These authors contributed equally to this work and*
[*]*e-mail: nyao@fas.harvard.edu*
(Dated: January 2, 2011)

Robust Quantum State Transfer in Unpolarized Spin Chains

Spin Chain

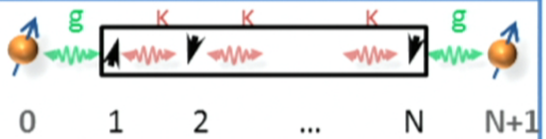

$H = H_0 + H_1$

κ>>g

$$H_0 = \sum_{j=1}^{N-1} \kappa (S_i^+ S_{i+1}^- + S_i^- S_{i+1}^+) + \frac{E_0}{2}\left(S_0^z + S_{N+1}^z\right)$$

$$H_1 = g\left(S_0^+ S_1^- + S_{N-1}^+ S_N^- + h.c\right)$$

Yao, L.J., Gorshkov, Gong, Zhai, Duan, Lukin, PRL 106, 040505 (2011)

Robust Quantum State Transfer in Unpolarized Spin Chains

Spin Chain

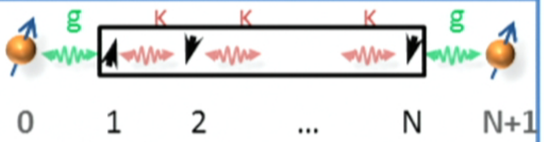

$H = H_0 + H_1$

κ>>g

$$H_0 = \sum_{j=1}^{N-1} \kappa (S_i^+ S_{i-1}^- + S_i^- S_{i-1}^-) + \frac{E_0}{2}\left(S_0^z + S_{N-1}^z\right)$$

$$H_1 = g\left(S_0^- S_1^- + S_{N-1}^- S_N^- + h.c\right)$$

Jordan-Wigner Transformation:

$$S_i^+ \approx c_i^\dagger,\ S_i^- \approx c_i,\ S_i^z \approx 2c_i^\dagger c_j - 1$$

Fermion Tunneling

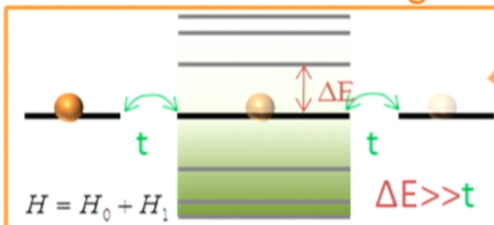

$H = H_0 + H_1$

ΔE>>t

$$H_0 = \sum_{k=1}^{N} E_k f_k^\dagger f_k + E_0\left(c_0^\dagger c_0 + c_{N-1}^\dagger c_{N-1}\right)$$

$$H_1 = \sum_{k=1}^{N} t_k \left(c_0^\dagger f_k + (-1)^{k-1} c_{N-1}^\dagger f_k + h.c.\right)$$

Yao, L.J., Gorshkov, Gong, Zhai, Duan, Lukin, PRL 106, 040505 (2011)

Robust Quantum State Transfer in Unpolarized Spin Chains

Spin Chain

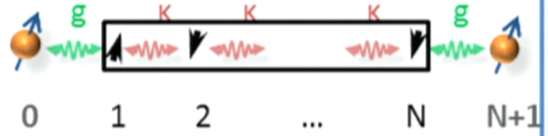

$H = H_0 + H_1$

κ>>g

$$H_0 = \sum_{j=1}^{N-1} \kappa (S_i^+ S_{i-1}^- + S_i^- S_{i-1}^-) + \frac{E_0}{2}\left(S_0^z + S_{N-1}^z\right)$$

$$H_1 = g\left(S_0^- S_1^- + S_{N-1}^- S_N^- + h.c\right)$$

Jordan-Wigner Transformation:

$$S_i^+ \approx c_i^\dagger, S_i^- \approx c_i, S_i^z \approx 2c_i^\dagger c_j - 1$$

Fermion Tunneling

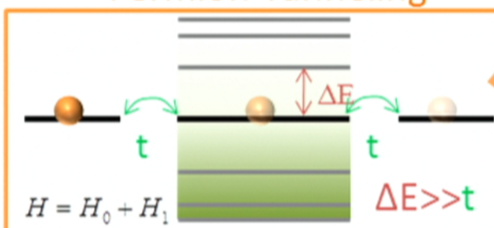

ΔE>>t

$H = H_0 + H_1$

$$H_0 = \sum_{k=1}^{N} E_k f_k^\dagger f_k + E_0\left(c_0^\dagger c_0 + c_{N-1}^\dagger c_{N-1}\right)$$

$$H_1 = \sum_{k=1}^{N} t_k \left(c_0^\dagger f_k + (-1)^{k-1} c_{N-1}^\dagger f_k + h.c.\right)$$

Unpolarized Spin-Chain for C-Phase Gate

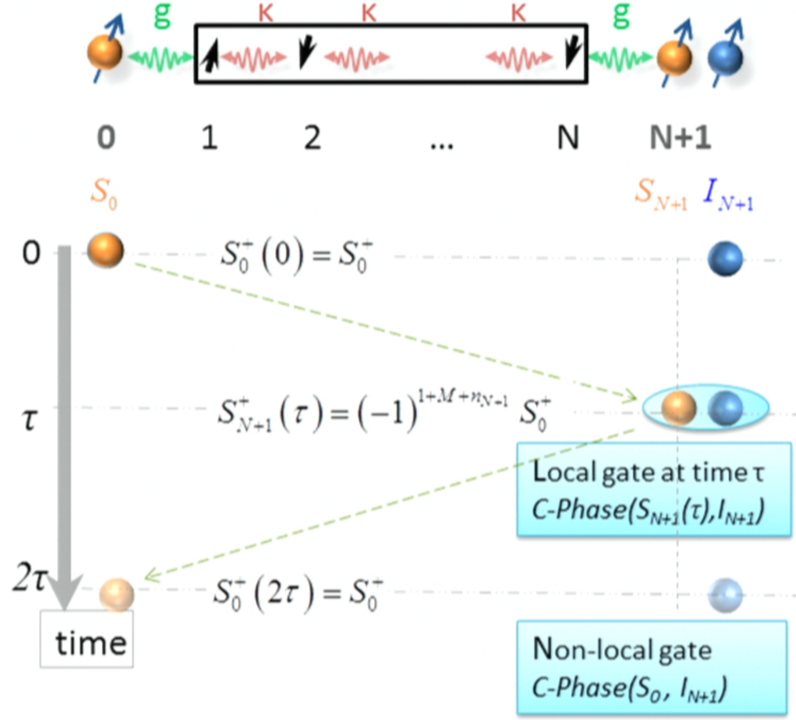

Yao, L.J., Gorshkov, Gong, Zhai, Duan, Lukin, PRL 106, 040505 (2011)

Summary: Spin Systems for QIP at Room Temperature

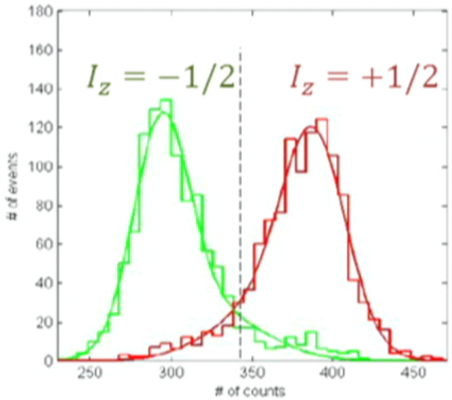

Good readout fidelity ≈ **92%**

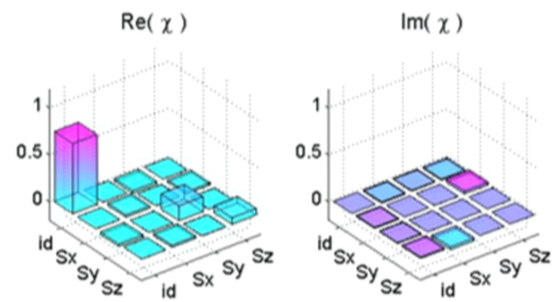

Good storage fidelity $F = (87 \pm 5)\%$
for 1 second storage time.

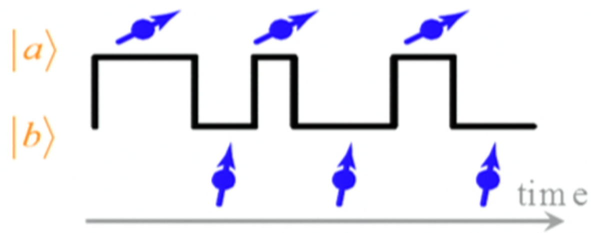

Motional Averaging to Improve Coherence
$\Gamma \approx \frac{\Delta\omega^2}{R}$ for $|\Delta\omega| \ll R$.

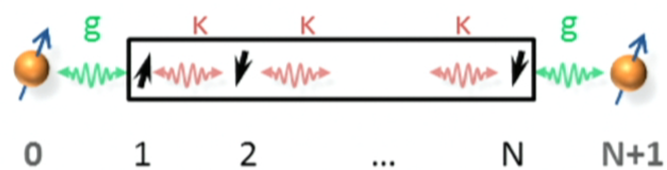

Quantum state transfer via Thermal Spin Chains.

Outline

1. Spin Systems for QIP (at Room Temperature)
   – Readout of a single nuclear spin
   – Nuclear spin quantum memory
   – Quantum state transfer via thermal spin chain
2. Topological Quantum Systems for QIP
   – Majorana fermions
   – Approaches to create & probe MFs
   – Hybrid platforms between topological and conventional quantum systems

Motivation

1. Conventional Quantum Systems
   - E.g., spins, ions, photons, SC devices, ...
   - Merits: universal gate set, distant entanglement, ...
   - Challenges: vulnerable to various imperfections

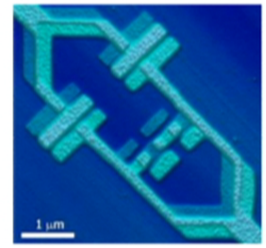

2. Topological Quantum Systems
   - E.g., Kitaev lattice model, FQHE, Topological Insulators, ...
   - Merits: robust against local decoherence.
   - Challenges: non-universal, hard to build a network ...

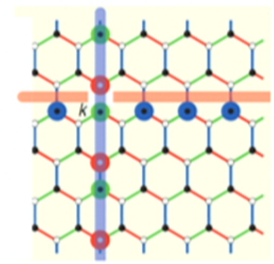

3. New Hybrid Systems
   - Combined merits from both systems
   - Network of topological quantum computers

TOPOLOGICAL QUANTUM SYSTEMS

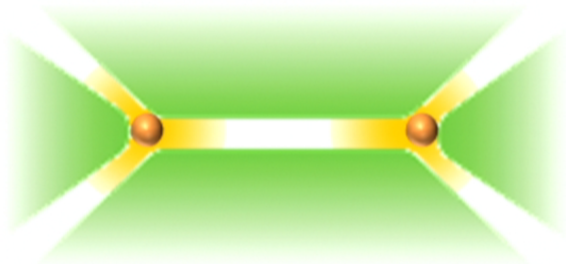

Majorana Fermions

- Majorana Fermions (MFs)
  - Fermion $\gamma_a \gamma_b = -\gamma_b \gamma_a$
  - Own anti-particle $\gamma = \gamma^\dagger$
  - E.g., "half of a Dirac Fermion" $\gamma_{2j-1} = \frac{c_j + c_j^\dagger}{2}$ and $\gamma_{2j} = \frac{c_j - c_j^\dagger}{2i}$

Ettore Majorana (1937)

Majorana Fermions

- Majorana Fermions (MFs)
  - Fermion $\gamma_a \gamma_b = -\gamma_b \gamma_a$
  - Own anti-particle $\gamma = \gamma^\dagger$
  - E.g., "half of a Dirac Fermion" $\gamma_{2j-1} = \dfrac{c_j + c_j^\dagger}{2}$ and $\gamma_{2j} = \dfrac{c_j - c_j^\dagger}{2i}$
- Search for MFs:

Ettore Majorana (1937)

P+ip SC (SrRuO)

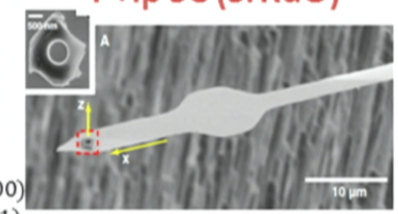

Read & Green, PRB (2000)
Jang, et al., Science (2011)

Topological Insulators

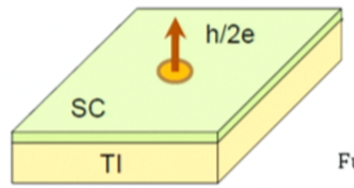

Fu & Kane. PRL (2008),

Quantum Wires

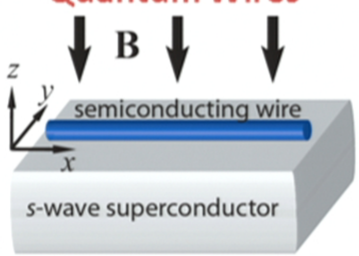

Lutchyn, et al., PRL (2010)
Oreg, et al., PRL (2010)
L.J., Pekker, et al., PRL (2011)

Cold Atoms

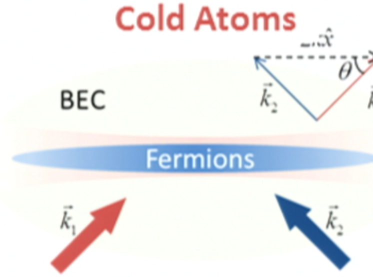

Sato, et al., PRL (2009)
Zhu, et al., PRL (2010)
L J, , Kitagawa, et al., PRL (2011)

Topological Qubit

- Four MFs encode 1 topological qubit
  - Subspace with odd Dirac fermion $\{|1\rangle_{12}|0\rangle_{34}, |0\rangle_{12}|1\rangle_{34}\}$.

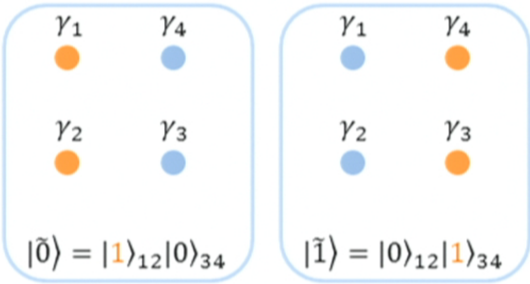

Topological Qubit

- Four MFs encode 1 topological qubit
  - Subspace with odd Dirac fermion $\{|1\rangle_{12}|0\rangle_{34}, |0\rangle_{12}|1\rangle_{34}\}$.
- Braiding of MFs
  - Non-abelian anyons

$$|\psi_{final}\rangle = U_{AB}|\psi_{init}\rangle$$

$$\text{with } U_{AB} = \frac{1}{\sqrt{2}}\begin{pmatrix} 1 & 1 \\ 1 & -1 \end{pmatrix}$$

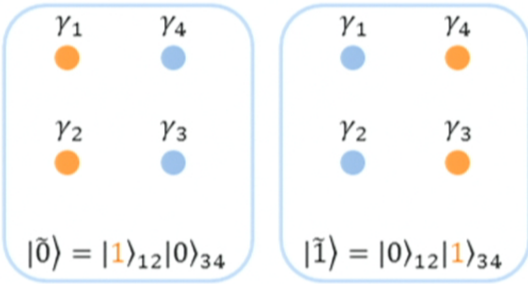

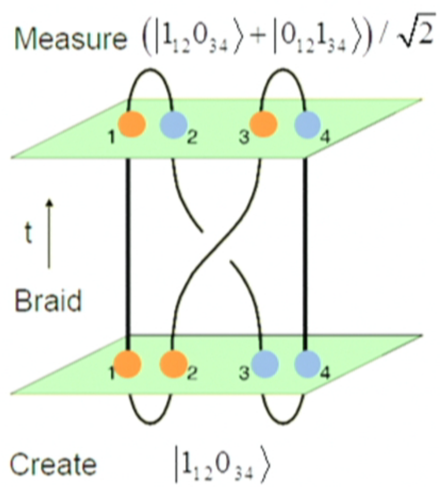

Kitaev Quantum Wire

-- Create "*half* of a Dirac Fermion"

Kitaev, arXiv: cond-mat/0010440 (2001).

Kitaev Quantum Wire
-- Create "*half* of a Dirac Fermion"

Kitaev, arXiv: cond-mat/0010440 (2001).

Kitaev Quantum Wire
-- Create "*half* of a Dirac Fermion"

Kitaev, arXiv: cond-mat/0010440 (2001).

Kitaev Quantum Wire
-- Create "*half* of a Dirac Fermion"

- Chain of (spinless) Dirac fermions

$$H = -\mu \sum_{j=1}^{N} c_j^\dagger c_j - \sum_{j=1}^{N-1} \left(t c_j^\dagger c_{j+1} + \Delta c_j c_{j+1} + h.c. \right)$$

Kitaev, arXiv: cond-mat/0010440 (2001).

Kitaev Quantum Wire

-- Create "*half* of a Dirac Fermion"

- Chain of (spinless) Dirac fermions

$$H = -\mu \sum_{j=1}^{N} c_j^\dagger c_j - \sum_{j=1}^{N-1} \left(t c_j^\dagger c_{j+1} + \Delta c_j c_{j+1} + h.c. \right)$$

- Introduce MFs:

$\gamma_{j,A} = \frac{c_j^\dagger + c_j}{2}$ and $\gamma_{j,B} = \frac{c_j^\dagger - c_j}{2i}$

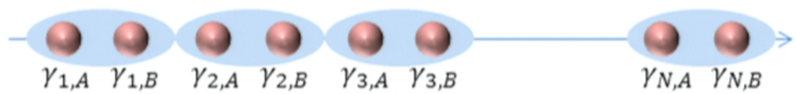

Kitaev, arXiv: cond-mat/0010440 (2001).

Kitaev Quantum Wire

-- Create "*half* of a Dirac Fermion"

- Chain of (spinless) Dirac fermions

$$H = -\mu \sum_{j=1}^{N} c_j^\dagger c_j - \sum_{j=1}^{N-1} \left(t c_j^\dagger c_{j+1} + \Delta c_j c_{j+1} + h.c. \right)$$

- Introduce MFs:

$$\gamma_{j,A} = \frac{c_j^\dagger + c_j}{2} \text{ and } \gamma_{j,B} = \frac{c_j^\dagger - c_j}{2i}$$

- Consider $\mu = 0$ and $t = \Delta$,

$$H = -it \sum_{j=1}^{N-1} \gamma_{j,B} \gamma_{j+1,A}$$

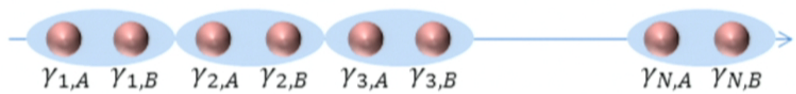

Kitaev, arXiv: cond-mat/0010440 (2001).

Kitaev Quantum Wire

-- Create "*half* of a Dirac Fermion"

- Chain of (spinless) Dirac fermions

$$H = -\mu \sum_{j=1}^{N} c_j^\dagger c_j - \sum_{j=1}^{N-1} \left(t c_j^\dagger c_{j+1} + \Delta c_j c_{j+1} + h.c. \right)$$

- Introduce MFs:

$\gamma_{j,A} = \frac{c_j^\dagger + c_j}{2}$ and $\gamma_{j,B} = \frac{c_j^\dagger - c_j}{2i}$

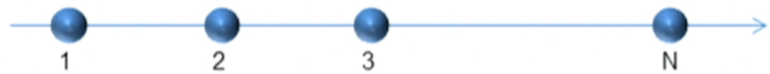

- Consider $\mu = 0$ and $t = \Delta$,

$$H = -it \sum_{j=1}^{N-1} \gamma_{j,B} \gamma_{j+1,A}$$

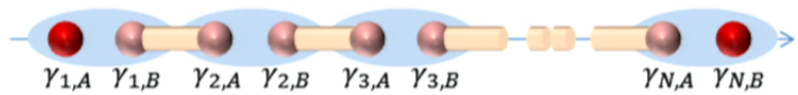

Kitaev, arXiv: cond-mat/0010440 (2001).

Kitaev Quantum Wire

-- Create "*half* of a Dirac Fermion"

- Chain of (spinless) Dirac fermions

$$H = -\mu \sum_{j=1}^{N} c_j^\dagger c_j - \sum_{j=1}^{N-1} \left(t c_j^\dagger c_{j+1} + \Delta c_j c_{j+1} + h.c. \right)$$

- Introduce MFs:

$$\gamma_{j,A} = \frac{c_j^\dagger + c_j}{2} \text{ and } \gamma_{j,B} = \frac{c_j^\dagger - c_j}{2i}$$

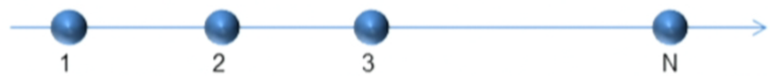

- Consider $\mu = 0$ and $t = \Delta$,

$$H = -it \sum_{j=1}^{N-1} \gamma_{j,B} \gamma_{j+1,A}$$

Two localized MFs at the end of the quantum wire!

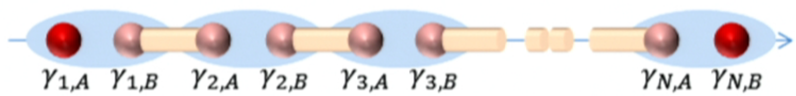

Kitaev, arXiv: cond-mat/0010440 (2001).

Kitaev Quantum Wire
-- Create "*half* of a Dirac Fermion"

- Chain of (spinless) Dirac fermions

$$H = -\mu \sum_{j=1}^{N} c_j^\dagger c_j - \sum_{j=1}^{N-1} \left(t c_j^\dagger c_{j-1} + \Delta c_j c_{j-1} + h.c. \right)$$

- Introduce MFs:

$$\gamma_{j,A} = \frac{c_j^\dagger + c_j}{2} \text{ and } \gamma_{j,B} = \frac{c_j^\dagger - c_j}{2i}$$

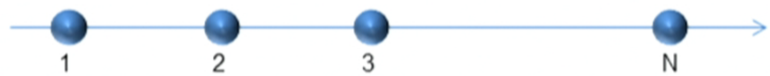

- Consider $\mu = 0$ and $t = \Delta$,

$$H = -it \sum_{j=1}^{N-1} \gamma_{j,B} \gamma_{j-1,A}$$

Two localized MFs at the end of the quantum wire!

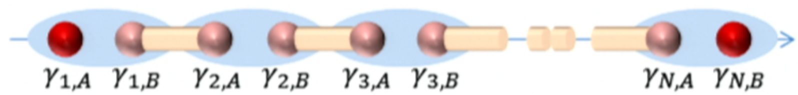

- For $|\mu| < 2t$, bound MFs exist! With exponential tail.

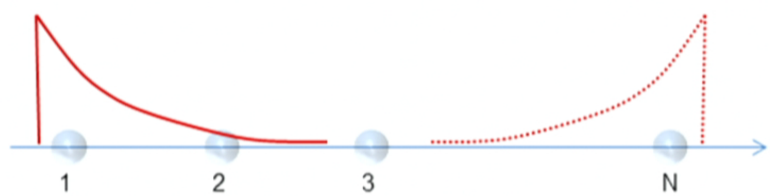

Kitaev, arXiv: cond-mat/0010440 (2001).

Topological Insulators

Interior: gapped insulator

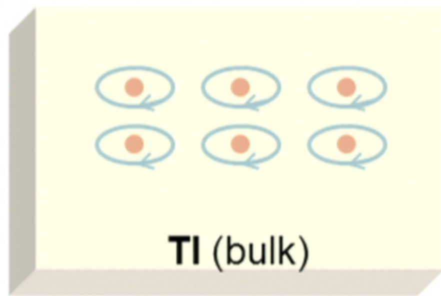

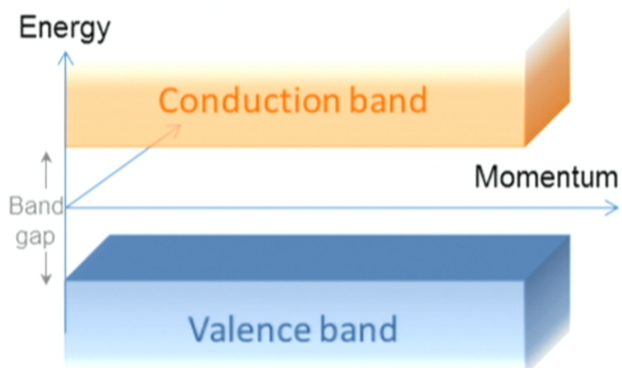

Surface: spin-locked conductor

$$H_{TI} = \psi^{\dagger}(v\vec{\sigma}\cdot\vec{p}-\mu)\psi$$

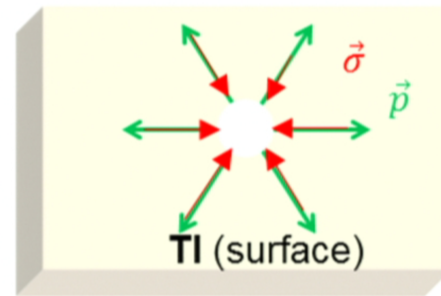

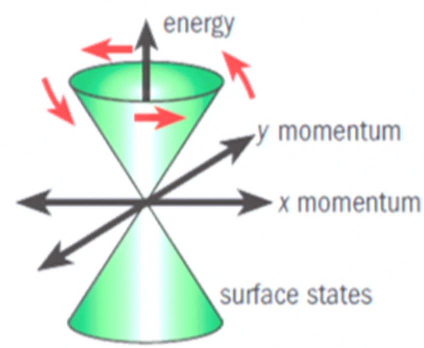

Hasan and Kane, RMP 82, 3045 (2010). C. Brüne, et al., Phys. Rev. Lett. 106, 126803 (2011).

How to create MFs? – Tri-Junction

- Topological Insulator
  - Interior: gapped insulator
  - Surface: spin-locked conductor

$$H_{TI} = \psi^\dagger(v\vec{\sigma}\cdot\vec{p} - \mu)\psi$$

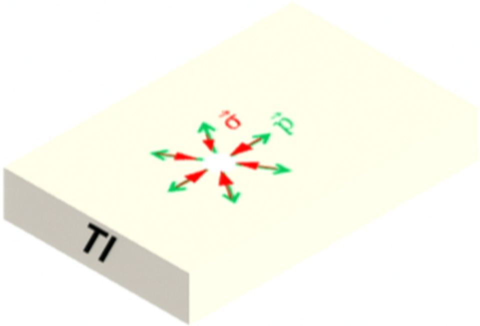

Fu and Kane, PRL 100, 096407 (2008)

How to create MFs? – Tri-Junction

- Topological Insulator
  - Interior: gapped insulator
  - Surface: spin-locked conductor

$$H_{TI} = \psi^\dagger(v\vec{\sigma}\cdot\vec{p} - \mu)\psi$$

- S-wave superconductor

$$H_S = \Delta\psi_\uparrow^\dagger\psi_\downarrow^\dagger + h.c.$$

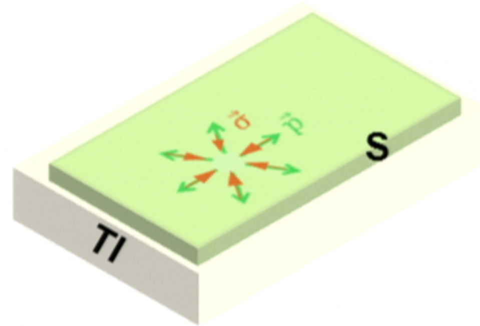

Fu and Kane, PRL 100, 096407 (2008)

How to create MFs? – Tri-Junction

- Topological Insulator
  - Interior: gapped insulator
  - Surface: spin-locked conductor

$$H_{TI} = \psi^\dagger(v\vec{\sigma}\cdot\vec{p} - \mu)\psi$$

- S-wave superconductor

$$H_S = \Delta\psi_\uparrow^\dagger\psi_\downarrow^\dagger + h.c.$$

- Similar to p+ip superconductor
  - Support MFs at vortices (e.g., Tri-Junction)

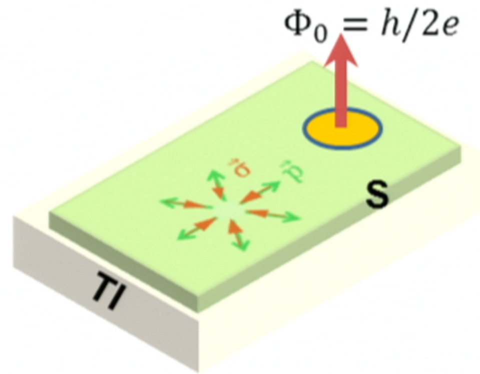

Fu and Kane, PRL 100, 096407 (2008)

How to create MFs? – Tri-Junction

- Topological Insulator
  - Interior: gapped insulator
  - Surface: spin-locked conductor

$$H_{TI} = \psi^\dagger(v\vec{\sigma}\cdot\vec{p} - \mu)\psi$$

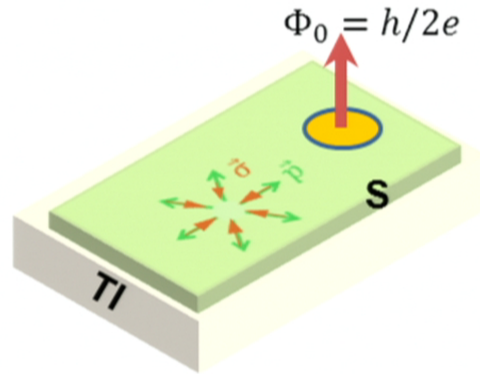

- S-wave superconductor

$$H_S = \Delta\psi_\uparrow^\dagger\psi_\downarrow^\dagger + h.c.$$

- Similar to p+ip superconductor
  - Support MFs at vortices (e.g., Tri-Junction)

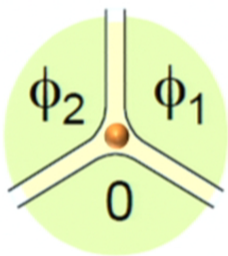

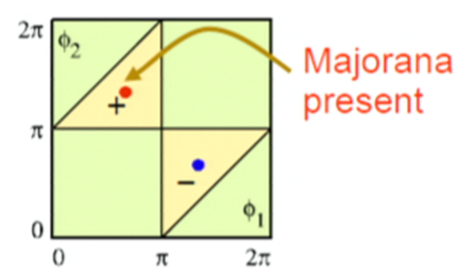

Fu and Kane, PRL 100, 096407 (2008)

Two MFs with Coupling

- Using two tri-junctions connected by a quantum wire
  - MF wavefunction controlled by ε
  - Interact along quantum wire

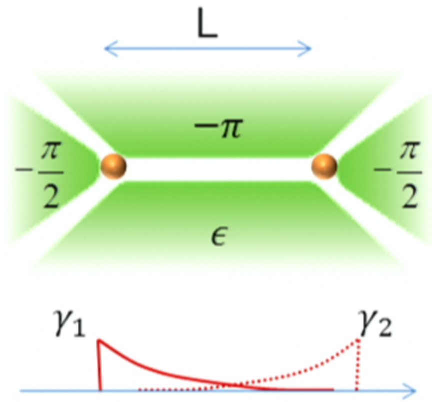

$$H_{wire} = -iv\tau^x \partial_x + \delta_\phi \tau^z$$

Fu and Kane, PRL 100, 096407 (2008)

Two MFs with Coupling

- Using two tri-junctions connected by a quantum wire
  - MF wavefunction controlled by ε
  - Interact along quantum wire

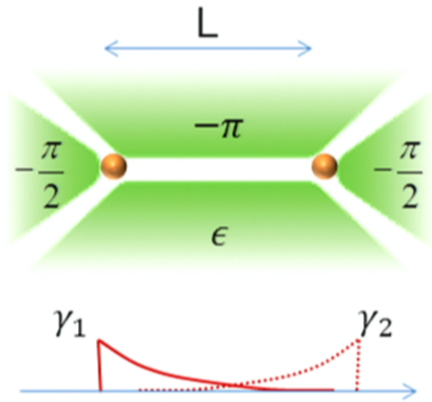

$$H_{wire} = -iv\tau^x\partial_x + \delta_\phi\tau^z$$

Fu and Kane, PRL 100, 096407 (2008)

Two MFs with Coupling

- Using two tri-junctions connected by a quantum wire
  - MF wavefunction controlled by ε
  - Interact along quantum wire

$$H_{12}^{MF} = iE(\varepsilon)\gamma_1\gamma_2 \cong E(\varepsilon) Z_{topo}$$

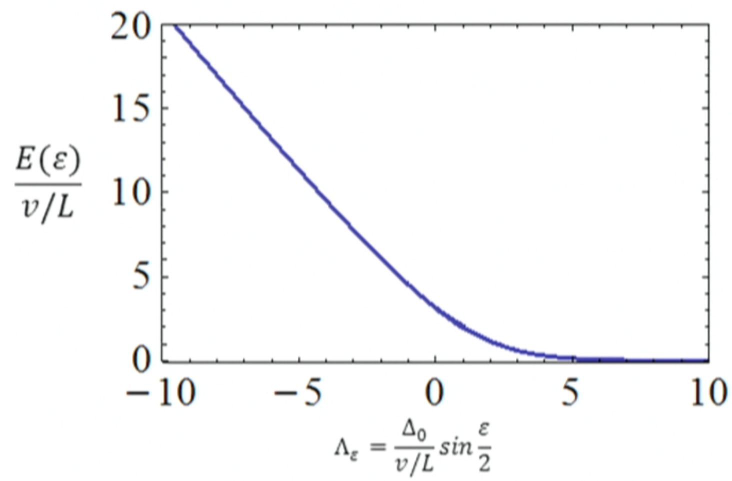

Fu and Kane, PRL 100, 096407 (2008)

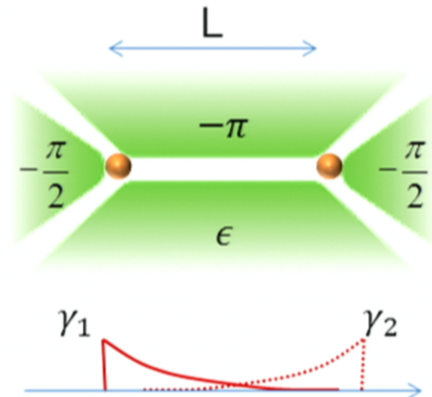

$$H_{wire} = -iv\tau^x\partial_x + \delta_\phi\tau^z$$

Two MFs with Coupling

- Using two tri-junctions connected by a quantum wire
  - MF wavefunction controlled by ε
  - Interact along quantum wire

$$H_{12}^{MF} = iE(\varepsilon)\gamma_1\gamma_2 \cong E(\varepsilon) Z_{topo}$$

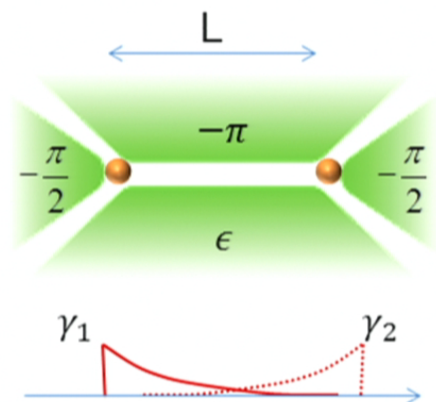

$$H_{wire} = -iv\tau^x\partial_x + \delta_\phi \tau^z$$

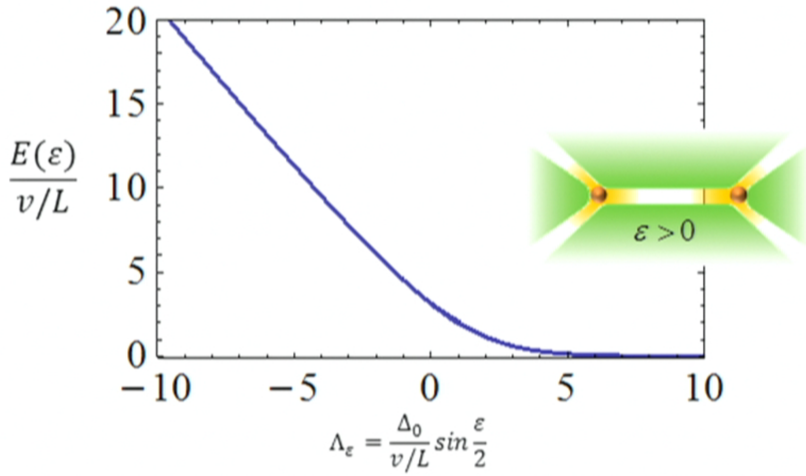

Fu and Kane, PRL 100, 096407 (2008)

Two MFs with Coupling

- Using two tri-junctions connected by a quantum wire
  - MF wavefunction controlled by ε
  - Interact along quantum wire

$$H_{12}^{MF} = iE(\varepsilon)\gamma_1\gamma_2 \cong E(\varepsilon)Z_{topo}$$

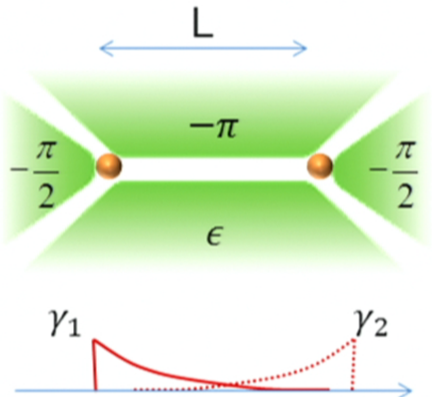

$$H_{wire} = -iv\tau^x\partial_x + \delta_\phi\tau^z$$

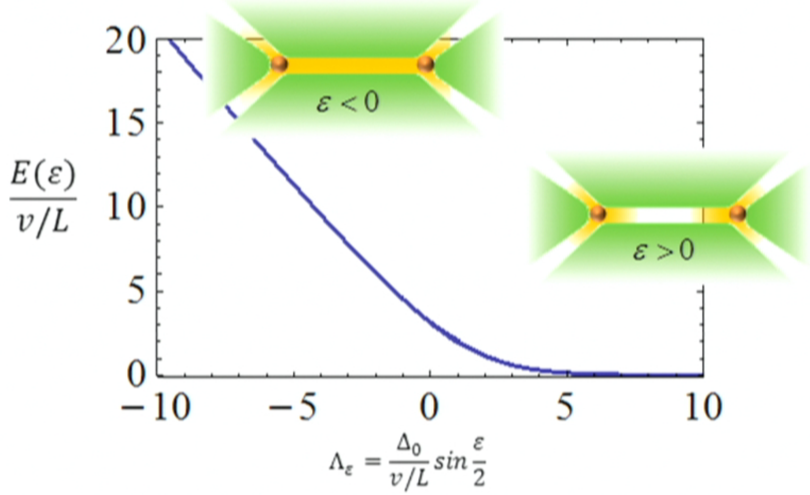

Fu and Kane, PRL 100, 096407 (2008)

Two MFs with Coupling

- Using two tri-junctions connected by a quantum wire
  - MF wavefunction controlled by ε
  - Interact along quantum wire

$$H_{12}^{MF} = iE(\varepsilon)\gamma_1\gamma_2 \cong E(\varepsilon)Z_{topo}$$

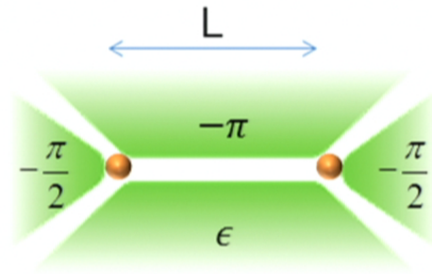

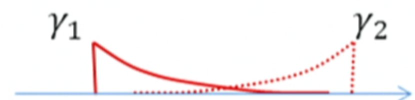

$$H_{wire} = -iv\tau^x\partial_x + \delta_\phi\tau^z$$

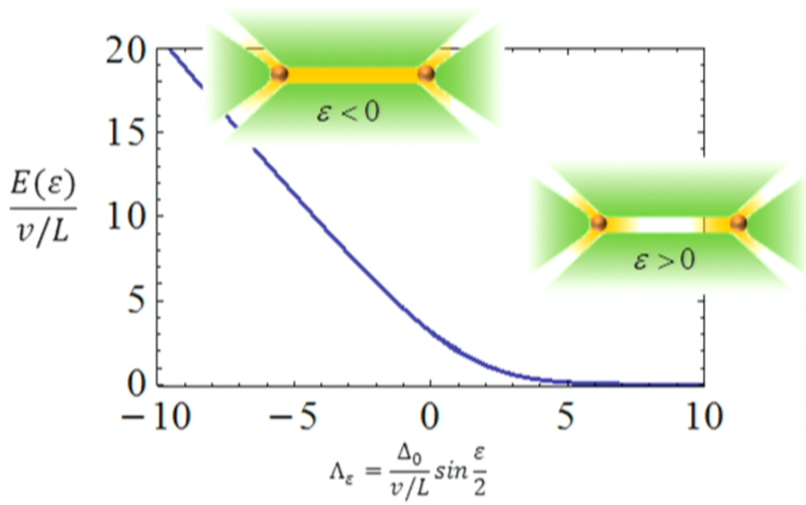

- Single qubit unitary gate:

$$U = e^{iH_{12}^{MF}t} = e^{i\theta Z_{topo}}$$

Fu and Kane, PRL 100, 096407 (2008)

Two MFs with Coupling

- Using two <u>tri-junctions</u> connected by a <u>quantum wire</u>
  - MF wavefunction controlled by ε
  - Interact along quantum wire

$$H_{12}^{MF} = iE(\varepsilon)\gamma_1\gamma_2 \cong E(\varepsilon) Z_{topo}$$

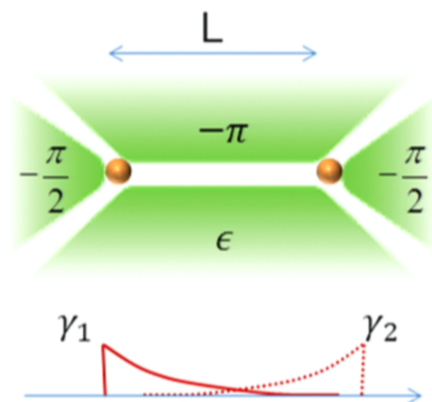

$$H_{wire} = -iv\tau^x\partial_x + \delta_\phi\tau^z$$

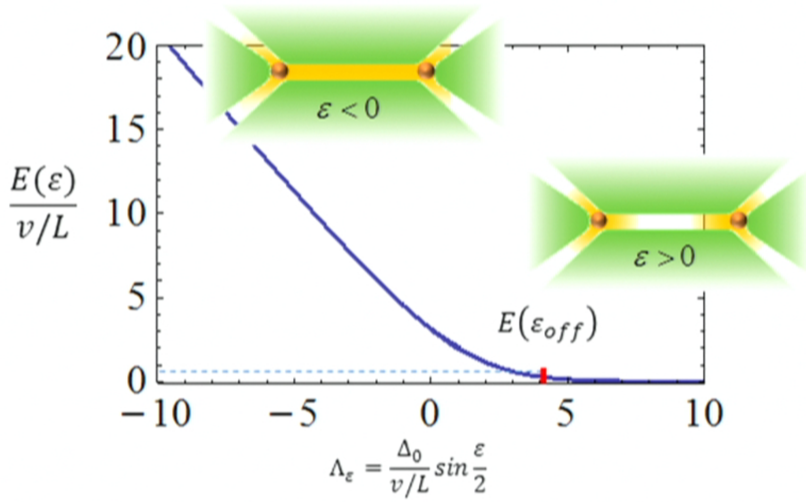

- Single qubit unitary gate:

$$U = e^{iH_{12}^{MF}t} = e^{i\theta Z_{topo}}$$

- Universal set of operations

Fu and Kane, PRL 100, 096407 (2008)

Superposition of Evolutions

- Interaction between Two MFs
  - Overlap along quantum wire

$$H_{12}^{MF} = iE(\varepsilon)\gamma_1\gamma_2 \cong E(\varepsilon)Z_{topo}$$

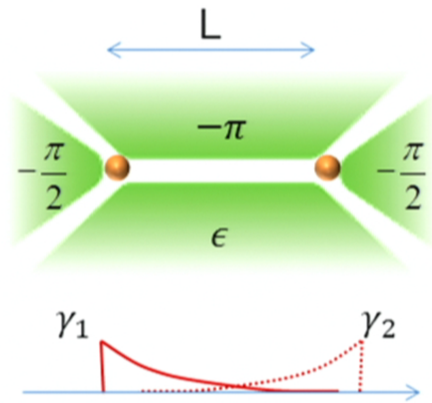

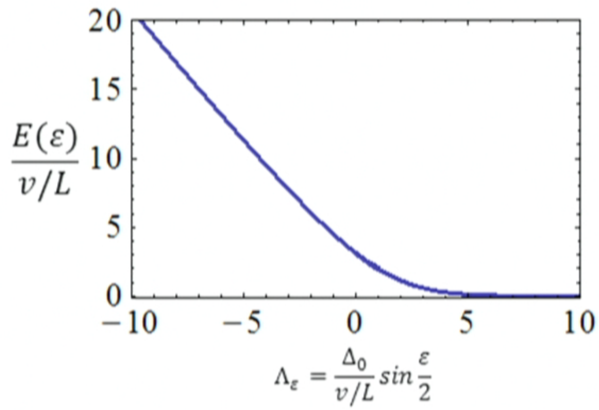

L.J., C. L. Kane and J. Preskill, PRL 106, 130504 (2011).

Superposition of Evolutions

- Interaction between Two MFs
  - Overlap along quantum wire

$$H_{12}^{MF} = iE(\varepsilon)\gamma_1\gamma_2 \cong E(\varepsilon)Z_{topo}$$

- Observation
  - $\hat{\varepsilon} \rightarrow |\varepsilon_0\rangle + |\varepsilon_1\rangle$ induces superposition of evolutions (i.e., Ctrl-Phase evolution)
  - Highly non-linear (good for switch on/off)

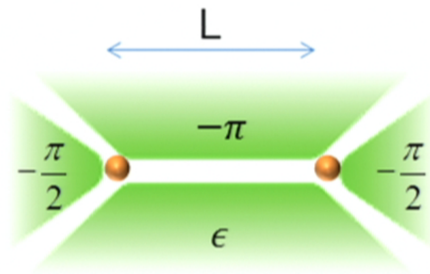

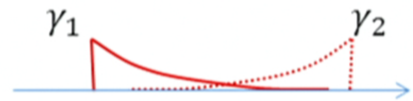

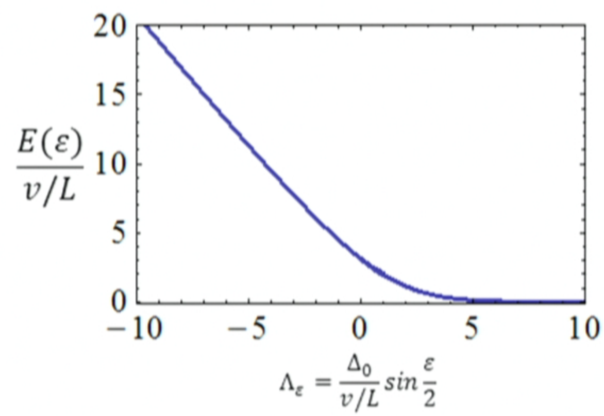

L.J., C. L. Kane and J. Preskill, PRL 106, 130504 (2011).

Superposition of Evolutions

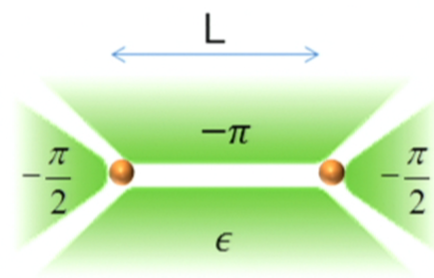

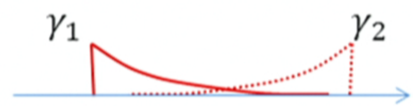

- Interaction between Two MFs
  - Overlap along quantum wire

$$H_{12}^{MF} = iE(\varepsilon)\gamma_1\gamma_2 \cong E(\varepsilon)Z_{topo}$$

- Observation
  - $\hat{\varepsilon} \rightarrow |\varepsilon_0\rangle + |\varepsilon_1\rangle$ induces superposition of evolutions (i.e., Ctrl-Phase evolution)
  - Highly non-linear (good for switch on/off)

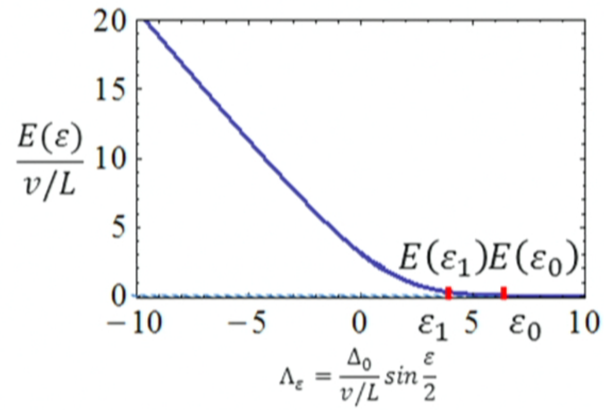

Switch off Interaction

L.J., C. L. Kane and J. Preskill, PRL 106, 130504 (2011).

Superposition of Evolutions

- Interaction between Two MFs
  - Overlap along quantum wire

    $$H_{12}^{MF} = iE(\varepsilon)\gamma_1\gamma_2 \cong E(\varepsilon)Z_{topo}$$

- Observation
  - $\hat{\varepsilon} \rightarrow |\varepsilon_0\rangle + |\varepsilon_1\rangle$ induces superposition of evolutions (i.e., Ctrl-Phase evolution)
  - Highly non-linear (good for switch on/off)

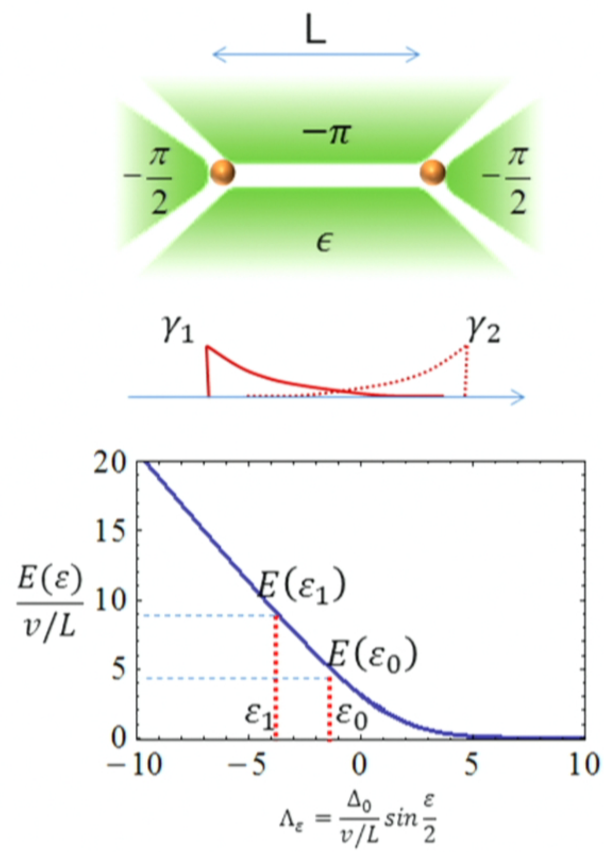

Switch on Interaction

L.J., C. L. Kane and J. Preskill, PRL 106, 130504 (2011).

Flux Qubit -- to achieve $|\varepsilon_0\rangle + |\varepsilon_1\rangle$

- Series of (three) Josephson Junctions
  - Josephson (potential) energy $U = -\sum_i E_{J,i} \cos\theta_i$
  - Charging (kinetic) energy $T = \frac{1}{2}\sum_i C_i V_i^2 = \frac{\Phi_0^2}{8\pi^2}\sum_i C_i \dot{\theta}_i^2$
  - Phase constraint $\sum_i \theta_i + 2f\pi \equiv 0 \,(\mathrm{mod}\, 2\pi)$

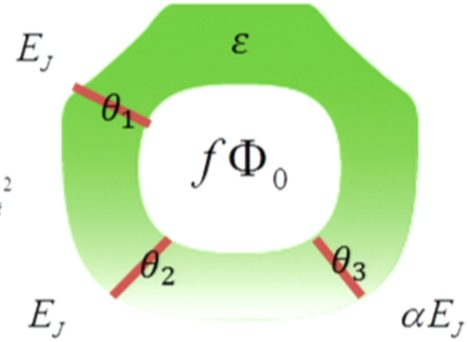

Flux Qubit -- to achieve $|\varepsilon_0\rangle + |\varepsilon_1\rangle$

- Series of (three) Josephson Junctions
  - Josephson (potential) energy $U = -\sum_i E_{J,i} \cos\theta_i$
  - Charging (kinetic) energy $T = \frac{1}{2}\sum_i C_i V_i^2 = \frac{\Phi_0^2}{8\pi^2}\sum_i C_i \dot{\theta}_i^2$
  - Phase constraint $\sum_i \theta_i + 2f\pi \equiv 0 \pmod{2\pi}$
  - Two potential minimum (1/2<α<1, f=1/2)

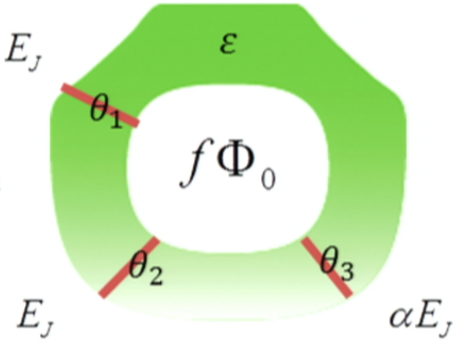

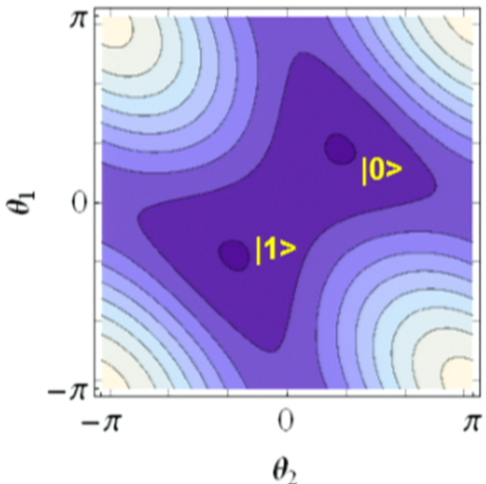

Flux Qubit -- to achieve $|\varepsilon_0\rangle + |\varepsilon_1\rangle$

- Series of (three) Josephson Junctions
  - Josephson (potential) energy $U = -\sum_i E_{J,i} \cos\theta_i$
  - Charging (kinetic) energy $T = \frac{1}{2}\sum_i C_i V_i^2 = \frac{\Phi_0^2}{8\pi^2}\sum_i C_i \dot{\theta}_i^2$
  - Phase constraint $\sum_i \theta_i + 2f\pi \equiv 0 \pmod{2\pi}$
  - Two potential minimum (1/2<α<1, f=1/2)

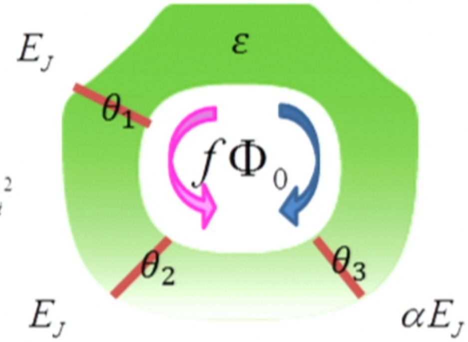

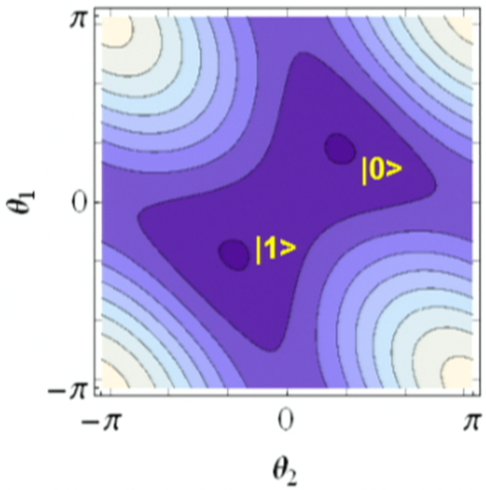

- SC Flux Qubit
  - CW/CCW current
  - Superposition of two values of ε
  - But, too large difference

Flux Qubit -- to achieve $|\varepsilon_0\rangle + |\varepsilon_1\rangle$

- Add a **fourth** junction ($\beta \gg 1$)
  - Josephson (potential) energy $U = -\sum_i E_{J,i} \cos\theta_i$
  - Charging (kinetic) energy $T = \frac{1}{2}\sum_i C_i V_i^2 = \frac{\Phi_0^2}{8\pi^2}\sum_i C_i \dot{\theta}_i^2$
  - Phase constraint $\sum_i \theta_i + 2f\pi \equiv 0 \pmod{2\pi}$

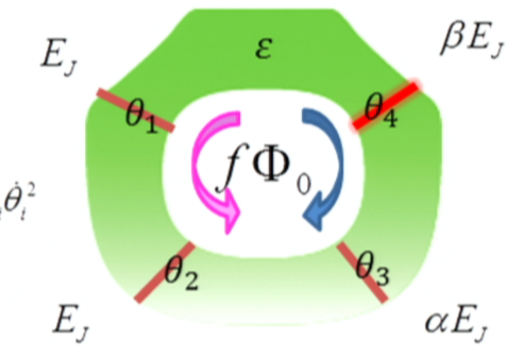

- SC Flux Qubit
  - CW/CCW current
  - Superposition of two values of ε

Flux Qubit -- to achieve $|\varepsilon_0\rangle + |\varepsilon_1\rangle$

- Add a **fourth** junction ($\beta \gg 1$)
  - Josephson (potential) energy $U = -\sum_i E_{J,i} \cos\theta_i$
  - Charging (kinetic) energy $T = \frac{1}{2}\sum_i C_i V_i^2 = \frac{\Phi_0^2}{8\pi^2}\sum_i C_i \dot{\theta}_i^2$
  - Phase constraint $\sum_i \theta_i + 2f\pi \equiv 0 \pmod{2\pi}$

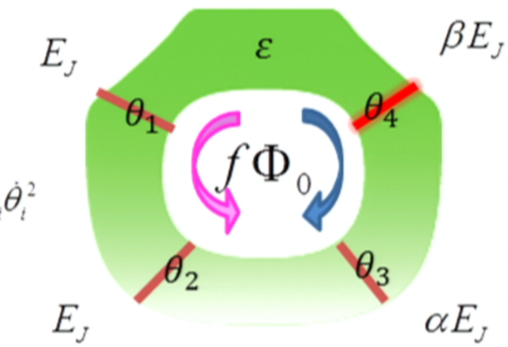

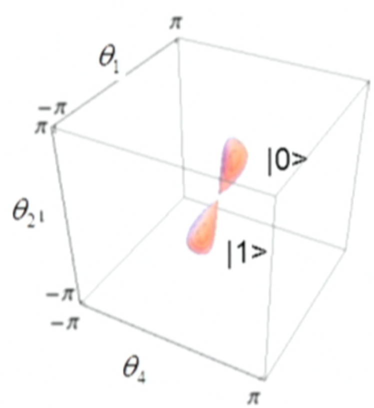

- SC Flux Qubit
  - CW/CCW current
  - Superposition of two values of ε

Flux Qubit -- to achieve $|\varepsilon_0\rangle + |\varepsilon_1\rangle$

- Add a **fourth** junction ($\beta \gg 1$)
  - Josephson (potential) energy $U = -\sum_i E_{J,i} \cos\theta_i$
  - Charging (kinetic) energy $T = \frac{1}{2}\sum_i C_i V_i^2 = \frac{\Phi_0^2}{8\pi^2}\sum_i C_i \dot{\theta}_i^2$
  - Phase constraint $\sum_i \theta_i + 2f\pi \equiv 0 \,(\mathrm{mod}\, 2\pi)$

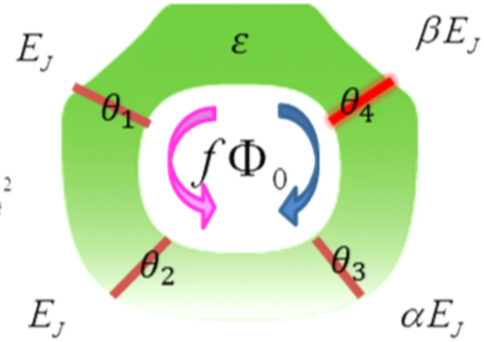

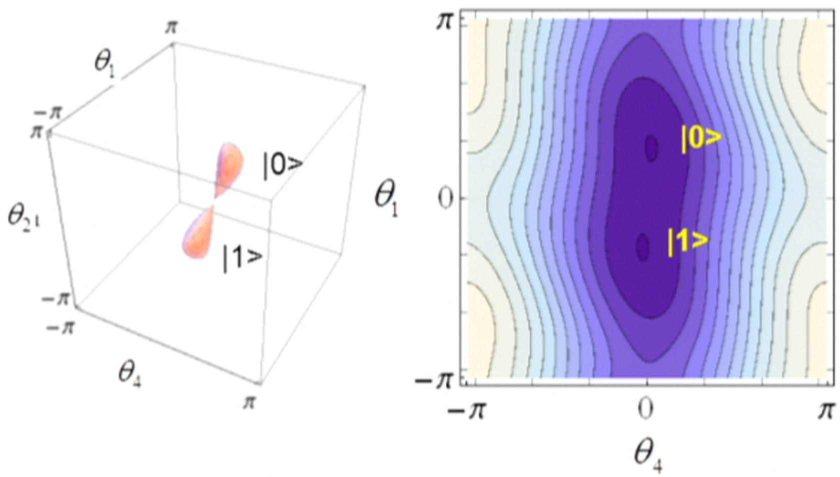

- SC Flux Qubit
  - CW/CCW current
  - Superposition of two values of ε

Hybrid System

- Topological Quantum Wire
  & Flux Qubit

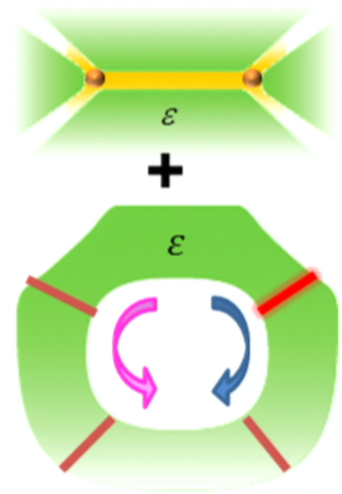

Hybrid System

- Topological Quantum Wire & Flux Qubit
- ε coherently controls the coupling between MFs:

$$H_{12}^{MF} \Rightarrow \begin{cases} E(\varepsilon_0) Z_{topo} & \text{for } \varepsilon=\varepsilon_0 \text{ with } |0\rangle_{flux} \\ E(\varepsilon_1) Z_{topo} & \text{for } \varepsilon=\varepsilon_1 \text{ with } |1\rangle_{flux} \end{cases}$$

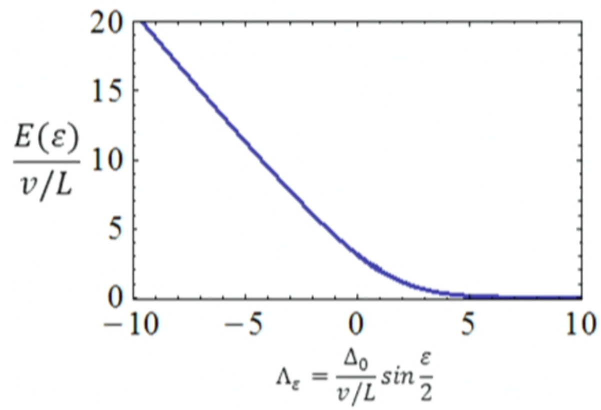

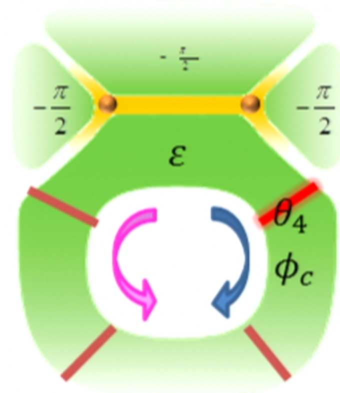

Quantum Fluctuations

Quantum Description of SC phase

$$\hat{\varepsilon} \approx \phi_c + \boldsymbol{\Delta\varepsilon} \cdot Z_{flux} + \delta\varepsilon \cdot (a^\dagger + a)$$

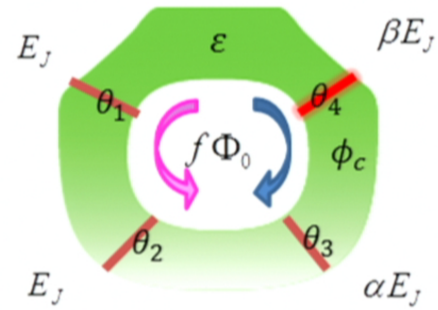

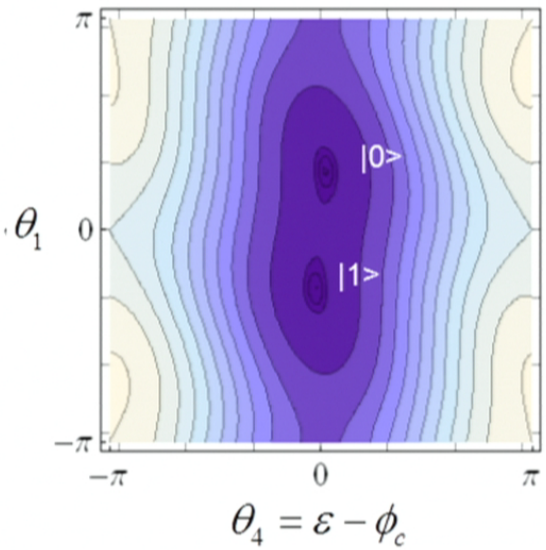

Hybrid System

- Topological Quantum Wire & Flux Qubit
- ε coherently controls the coupling between MFs:

$$H_{12}^{MF} \Rightarrow \begin{cases} E(\varepsilon_0) Z_{topo} & \text{for } \varepsilon=\varepsilon_0 \text{ with } |0\rangle_{flux} \\ E(\varepsilon_1) Z_{topo} & \text{for } \varepsilon=\varepsilon_1 \text{ with } |1\rangle_{flux} \end{cases}$$

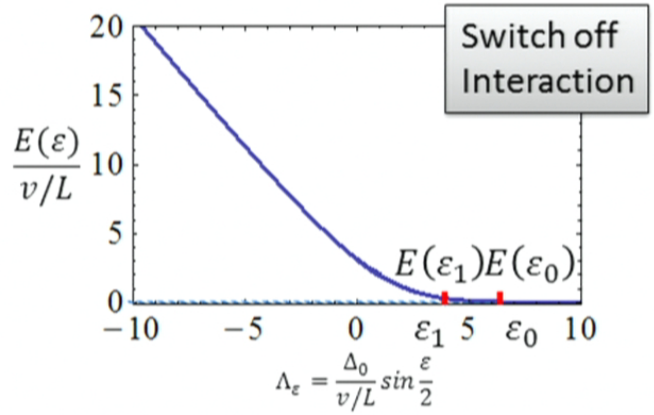

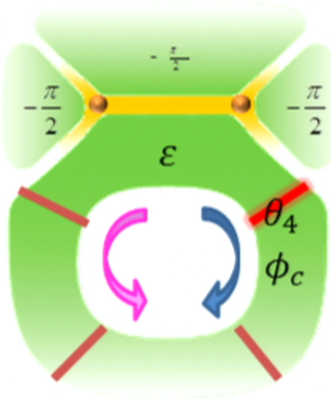

Quantum Fluctuations

Quantum Description of SC phase

$$\hat{\varepsilon} \approx \phi_c + \boldsymbol{\Delta\varepsilon} \cdot Z_{flux} + \delta\varepsilon \cdot (a^\dagger + a)$$

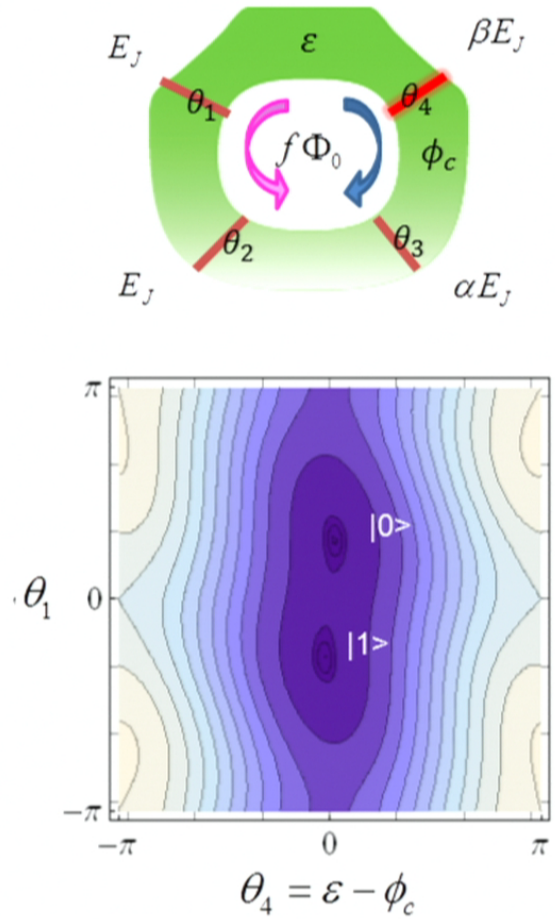

Quantum Fluctuations

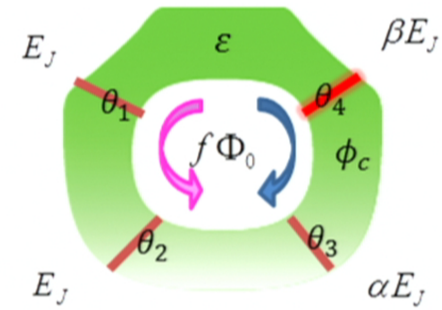

Quantum Description of SC phase

$$\hat{\varepsilon} \approx \phi_c + \boldsymbol{\Delta\varepsilon} \cdot Z_{flux} + \boldsymbol{\delta\varepsilon} \cdot (a^\dagger + a)$$

Harmonic oscillator model

- Oscillator frequency: $\omega = \sqrt{8E_J E_C}$
- Quantum fluctuation: $\delta\varepsilon \approx \frac{1}{\sqrt{\beta}}\left(\frac{8E_C}{E_J}\right)^{1/4} \propto \beta^{-1/2}$
- Phase separation: $\Delta\varepsilon \approx \frac{1}{\beta}\sqrt{1 - \frac{1}{4\alpha^2}} \propto \beta^{-1}$

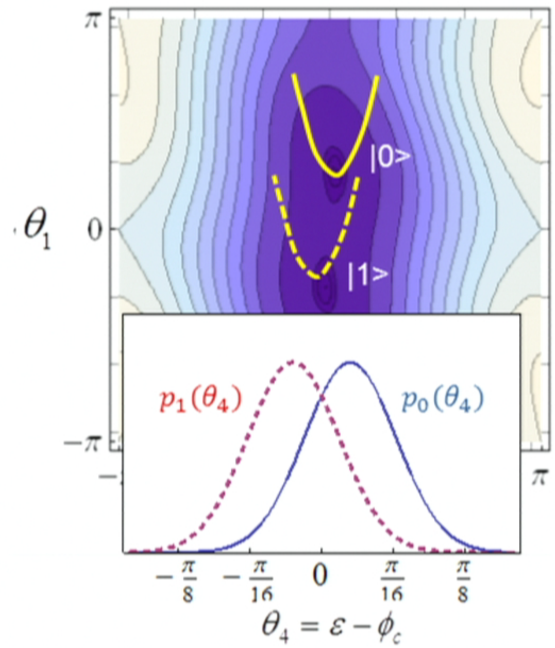

Quantum Fluctuations

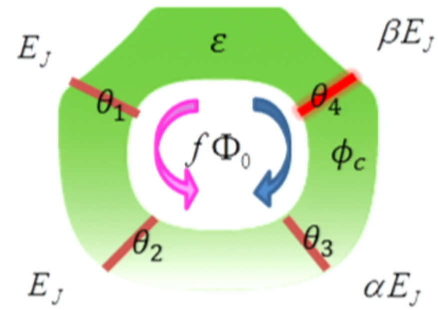

Quantum Description of SC phase

$$\hat{\varepsilon} \approx \phi_c + \boldsymbol{\Delta\varepsilon} \cdot Z_{flux} + \boldsymbol{\delta\varepsilon} \cdot (a^\dagger + a)$$

Harmonic oscillator model

- Oscillator frequency: $\omega = \sqrt{8E_J E_C}$
- Quantum fluctuation: $\delta\varepsilon \approx \frac{1}{\sqrt{\beta}}\left(\frac{8E_C}{E_J}\right)^{1/4} \propto \beta^{-1/2}$
- Phase separation: $\Delta\varepsilon \approx \frac{1}{\beta}\sqrt{1 - \frac{1}{4\alpha^2}} \propto \beta^{-1}$

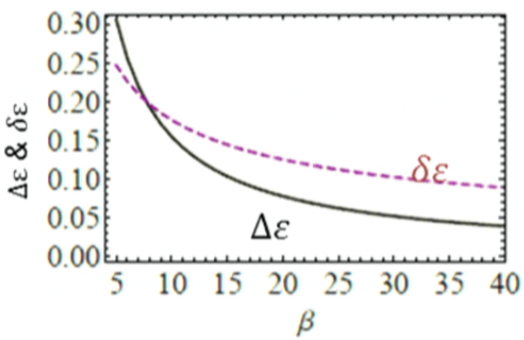

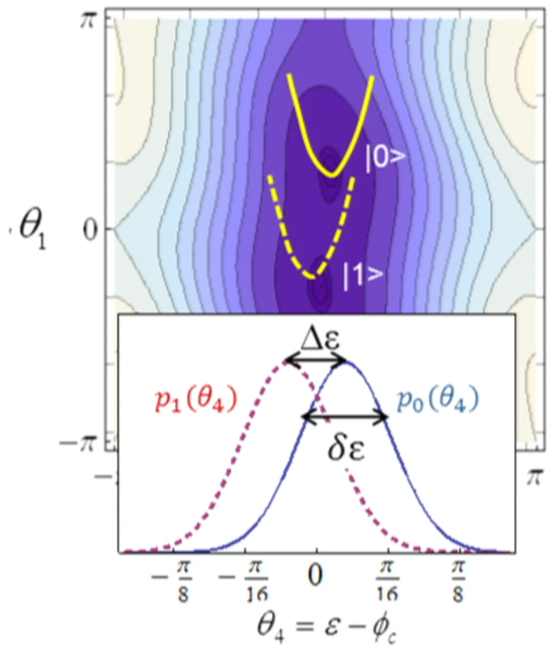

Coupling Hamiltonian

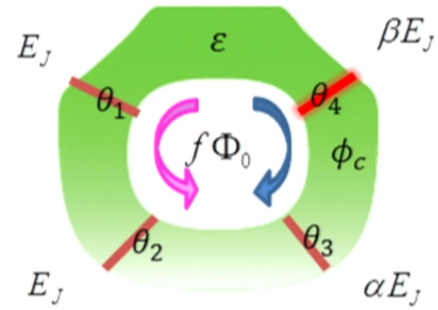

- Quantum Description of SC phase

$$\hat{\varepsilon} \approx \phi_c + \Delta\varepsilon \cdot Z_{flux} + \delta\varepsilon \cdot \left(a^\dagger + a\right)$$

- MF Hamiltonian

$$H = E\left(\hat{\varepsilon}\right) Z_{topo} \approx \left\langle E\left(\hat{\varepsilon}\right)\right\rangle_{G.S.} Z_{topo}$$

$$= \left(\left\langle E_0\right\rangle |0\rangle\langle 0| + \left\langle E_1\right\rangle |1\rangle\langle 1|\right)_{flux} \otimes Z_{topo}$$

with $\left\langle E_{0/1}\right\rangle \equiv \int E(\varepsilon)\, p_{0/1}(\varepsilon - \phi_c)\, d\varepsilon$

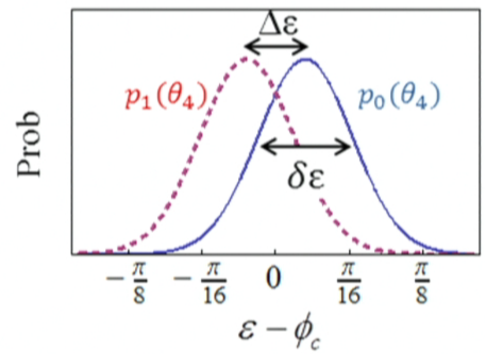

- Coupling for Controlled-Phase Gate

$$H_I = \frac{g}{4} Z_{flux} Z_{topo}$$

with coupling strength

$$g \approx \left(E(\varepsilon_1) - E(\varepsilon_0)\right) + \frac{1}{4}\left(E''(\varepsilon_1) - E''(\varepsilon_0)\right)\delta\varepsilon^2 + \ldots$$

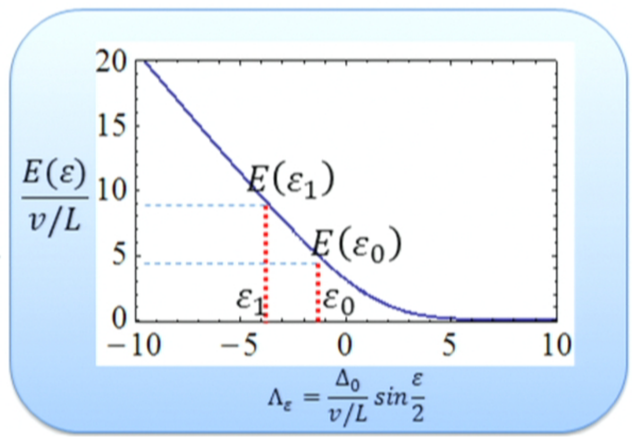

Transfer Quantum Information

- QND Repetitive measurement

Topo qubit:. $|0\rangle, |1\rangle$ — $Z_f Z_t$

Flux qubit: $|0\rangle + |1\rangle$ — [measurement] $|0\rangle \pm |1\rangle$

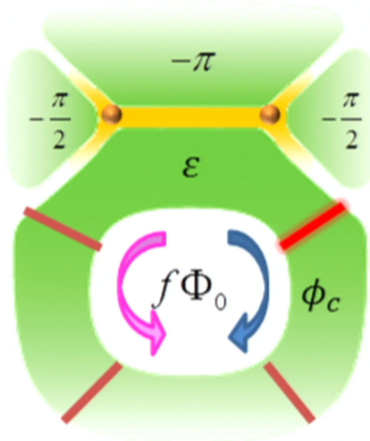

Transfer Quantum Information

- QND Repetitive measurement

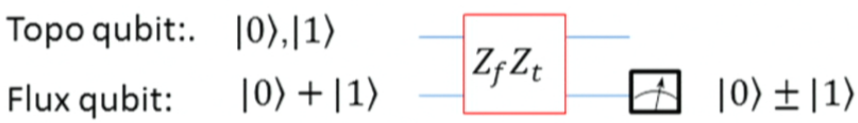

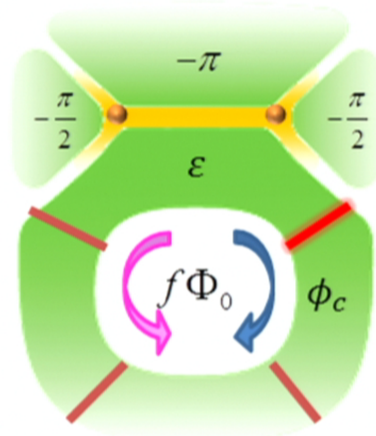

- **SWAP** quantum state between topological qubit to flux qubit

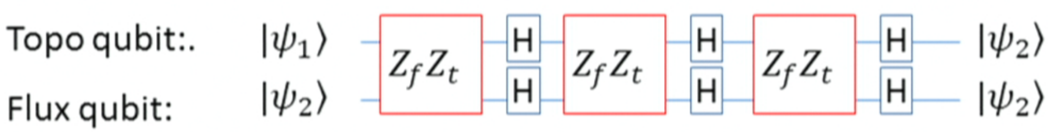

Imperfections

- Flux qubit tunneling $\eta_{tunnel} \approx (t/g)^2$
- Oscillator excitation $\eta_{exc} \approx (g/\omega)^2$
- Finite length L $\eta_L \approx e^{-KL}$
- Thermal excitation $\eta_{th} \approx e^{-v_F/(Lk_B T)}$

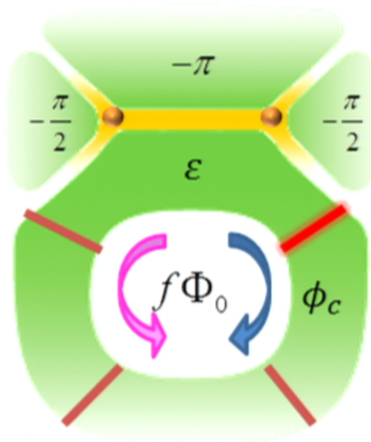

Imperfections

- Flux qubit tunneling $\eta_{tunnel} \approx (t/g)^2$
- Oscillator excitation $\eta_{exc} \approx (g/\omega)^2$
- Finite length L $\eta_L \approx e^{-KL}$
- Thermal excitation $\eta_{th} \approx e^{-v_F/(Lk_BT)}$

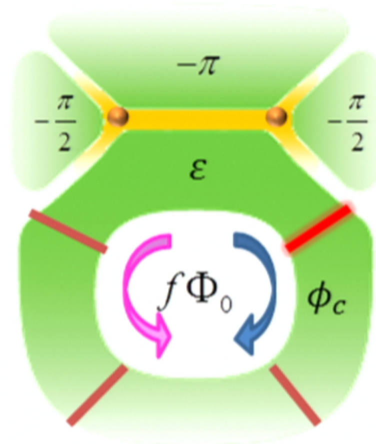

Possible to have $\eta < 10^{-2}$, with parameters:

$$E_J = 200(2\pi)GHz, E_C = 2.5(2\pi)GHz, \alpha = 0.8, \beta = 10$$
$$\Rightarrow \Delta\varepsilon \sim \delta\varepsilon \sim 0.1\ rad$$

$$L \approx 5\mu m,\ v_F \approx 10^5 m/s,\ \Delta_0 \approx 0.1meV, T = 20mK$$
$$\Rightarrow \mathrm{g} \approx 0.2\text{~}2\ (2\pi)GHz,$$
$$\Rightarrow \omega \gg g \gg t \gg 1/T_2$$

with $\omega \approx 60(2\pi)GHz, t \approx 70(2\pi)MHz, T_2 \approx 4\mu s.$

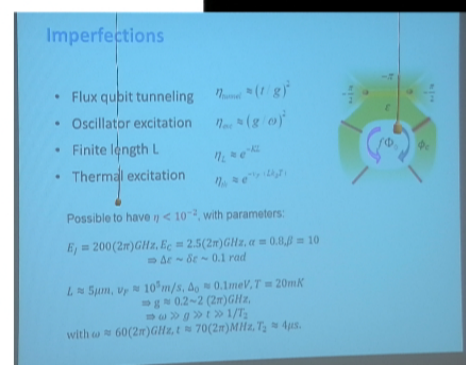

Summary

- Hybrid system of topological and flux qubits
  - Measure, probe anyonic statics, connect different topological systems, …
- Various related proposals
  - Semiconductor quantum wire + SC flux qubit using Aharonov-Casher effect
    - Hassler et al., NJP 12, 125002 (2010)
    - Bonderson, Lutchyn, PRL 106, 130505 (2011)
  - Toric code & cavity QED
    - Jiang, et al., Nature Physics 4, 482 (2008)

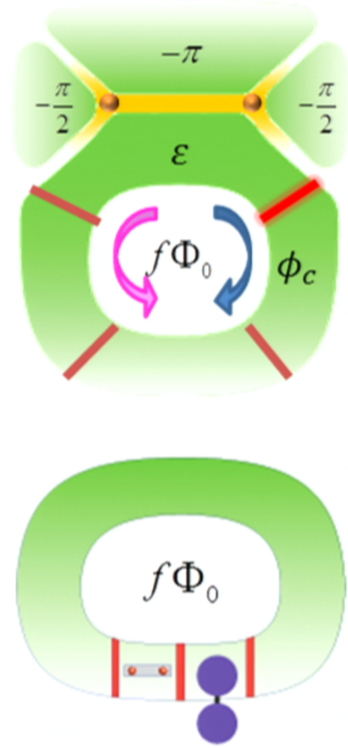

Summary

- Hybrid system of topological and flux qubits
  - Measure, probe anyonic statics, connect different topological systems, …
- Various related proposals
  - Semiconductor quantum wire + SC flux qubit using Aharonov-Casher effect
    - Hassler et al., NJP 12, 125002 (2010)
    - Bonderson, Lutchyn, PRL 106, 130505 (2011)
  - Toric code & cavity QED
    - Jiang, et al., Nature Physics 4, 482 (2008)
- Topological quantum networks
  - Optically connect topological systems

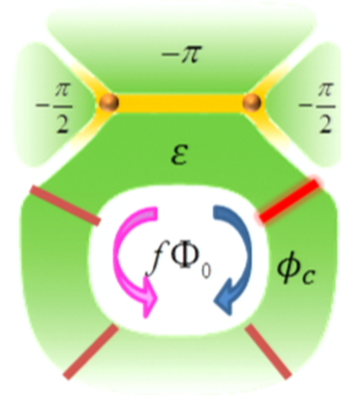

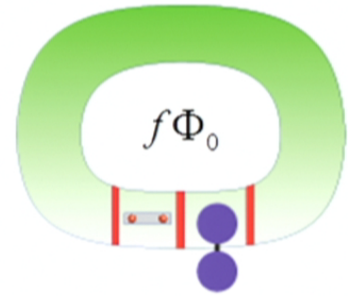

Summary of Other Results

Summary of Other Results

Scalable Architecture for Room Temperature Quantum computer

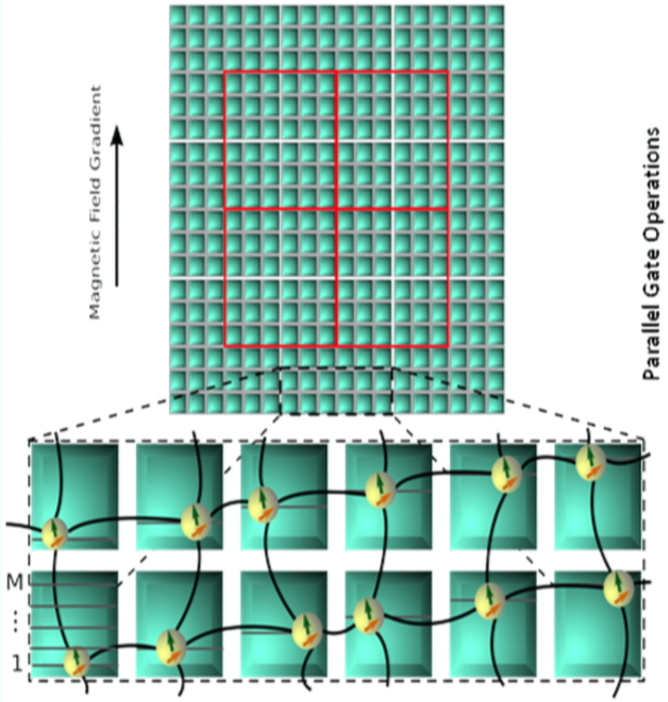

Parallel Gate Operations

Architecture based on control hierarchy:

Plaquette: 400nm x 400nm
- Single computational NV register
- Optical control and readout of individual registers

Super-plaquette: 10um x 10um
- 25 x 25 Plaquettes
- Confined microwaves manipulate individual super-plaquettes
- Parallel operations over all plaquettes

Super-plaquette Dual Lattice:
- Manipulate plaquette coupling across super-plaquette boundaries

Staggered NV array allows for individual addressing via 1D magnetic field gradient

Black lines represent DSCB mediated coherent coupling:

USC transfer to connect remote registers

N. Y. Yao, L.J., A. V. Gorshkov, P. Maurer, G. Giedke, I. Cirac and M. D. Lukin, arXiv: 1012.2864

Summary of Other Results

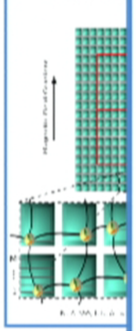

Universality of Nested Uhrig Dyanmical Decoupling

Nested Uhrig sequence

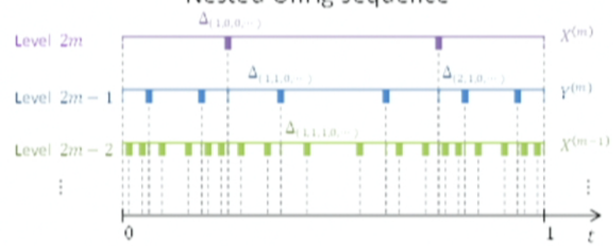

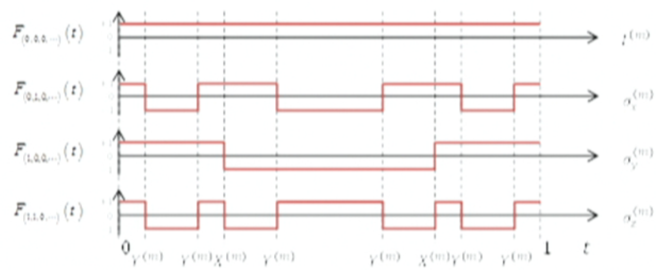

L. Jiang and A. Imambekov, arXiv: 1104.5021

Timing for the pulses

$$\Delta_l = \sin^2 \frac{l\pi}{2(N+1)}$$

$$\Delta_{(l_2,l_1)} = \Delta_{l_2} + \left(\Delta_{l_2+1} - \Delta_{l_2}\right)\Delta_{l_1}$$

$$\Delta_{(l_r,\cdots,l_1)} = \Delta_{l_r} + \left(\Delta_{l_r+1} - \Delta_{l_r}\right)\Delta_{(l_{r-1},\cdots,l_1)}$$

System-Bath Interaction is:

$$H(\tau) = \sum_\alpha \hat{S}_\alpha \otimes \hat{B}_\alpha(\tau)$$

Toggling frame Hamiltonian

$$\tilde{H}(\tau) = \sum_\alpha F_\alpha(\tau)\hat{S}_\alpha \otimes \hat{B}_\alpha(\tau)$$

Unitary Evolution

$$\tilde{U}(t) = T\exp\left[-i\int_0^t \tilde{H}(\tau)d\tau\right] = I \otimes U_B(t) + O(t^{N+1})$$

Summary of Other Results

Subwavelength Imaging & Control

-- Resolving two NV centers in diamond

Imaging
- Beyond diffraction limit
- Confocal not resolvable

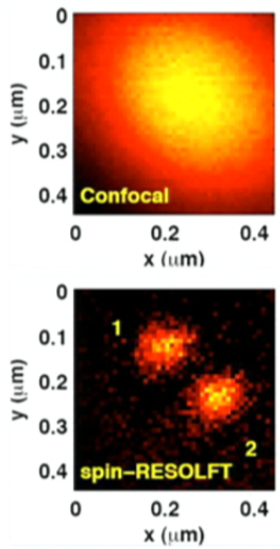

Control: Use quantum Zeno effect.

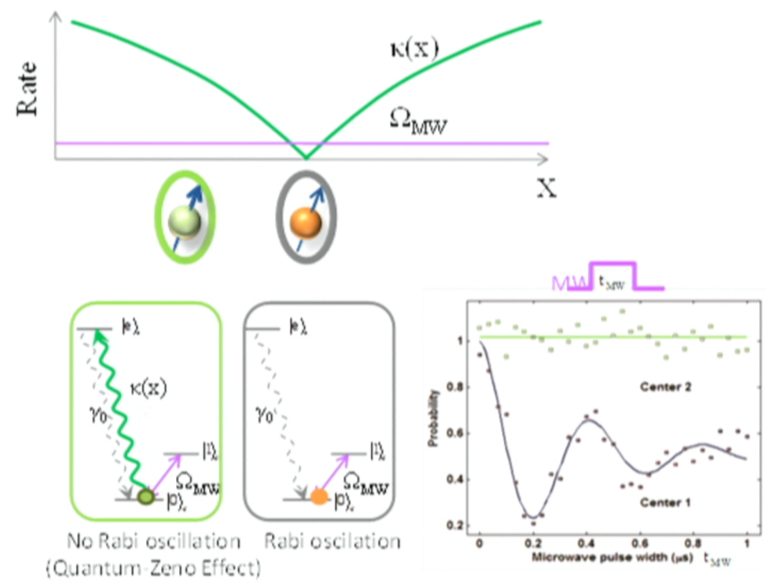

Maurer, Maze, Stanwix, LJ., Gorshkov, Zibrov, Harke, Hodges, Zibrov, Twitchen, Hell, Walsworth, Lukin, Nature Physics 6, 912 (2010).

Summary of Other Results

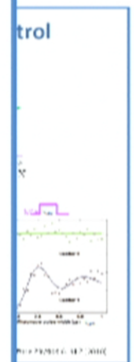

Verify Spin-Photon Entanglement

Energy levels of NV center

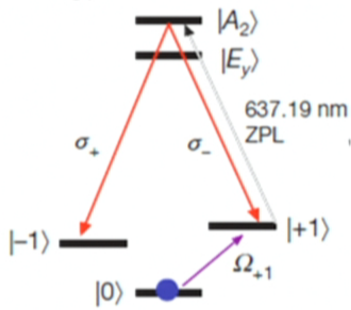

Entangled state between spin & photon

$$
\begin{aligned}
&|\Psi_{Bell}\rangle_{spin-photon} \\
&= |-1\rangle_s |R\rangle_p + |+1\rangle_s |L\rangle_p \\
&= |+\rangle_s |V\rangle_p + |-\rangle_s |H\rangle_p
\end{aligned}
$$

Experimental Results

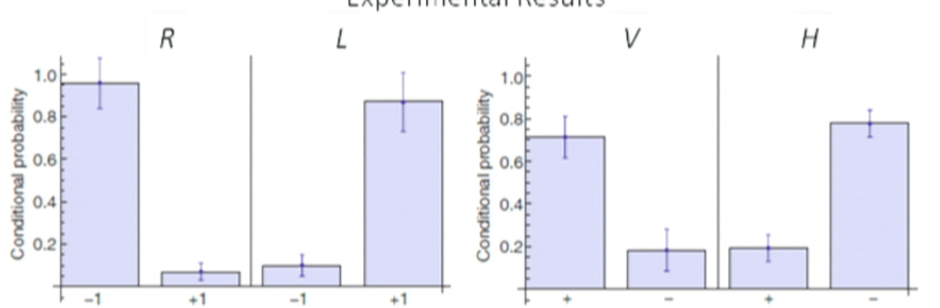

Togan, Chu, Trifonov, L.J., Maze, Childress, Dutt, Sorensen, Hemmer, Zibrov, Lukin, Nature 466, 730-734 (2010)

Summary of Other Results

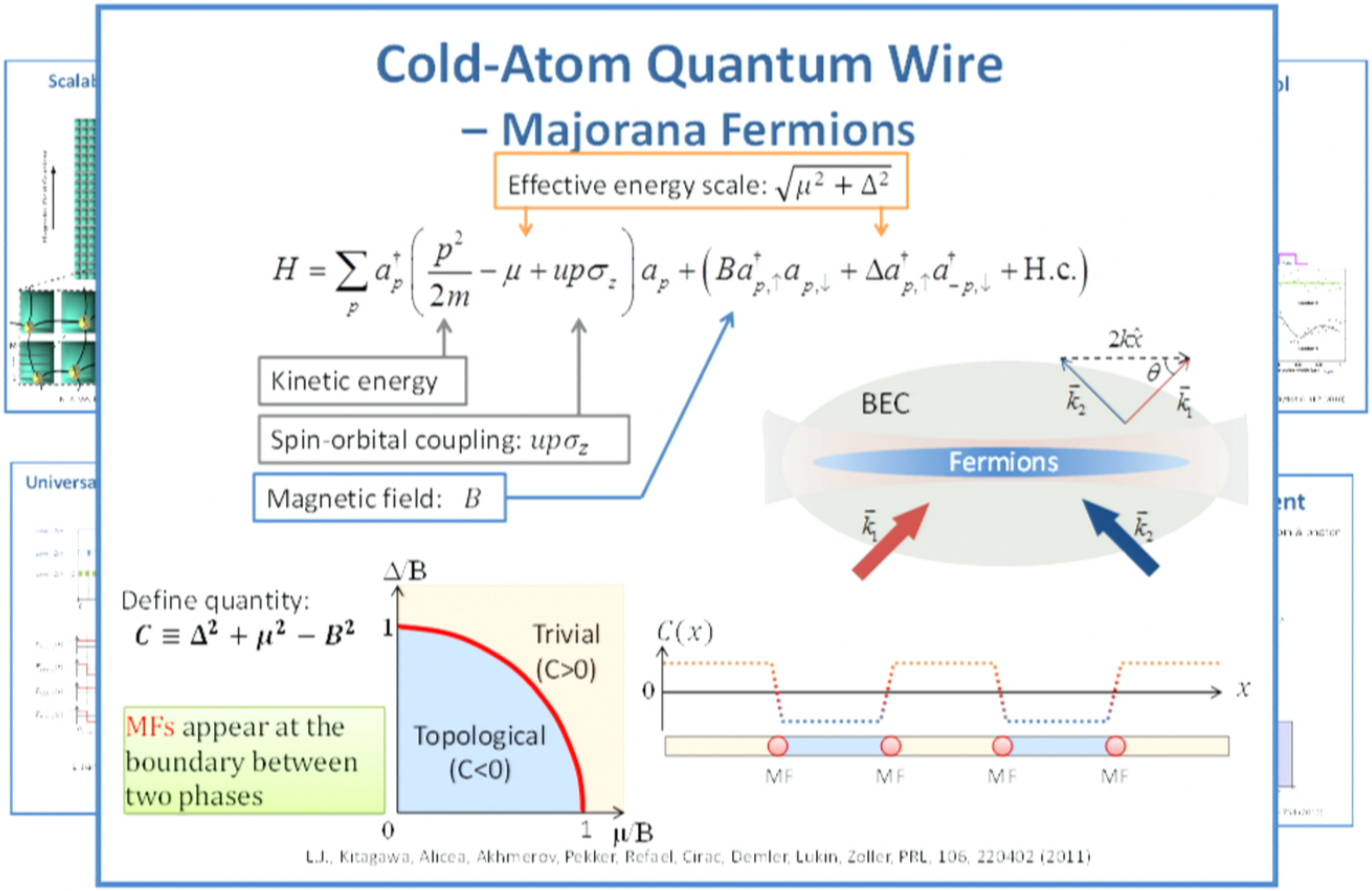

Summary of Other Results

Three-leg Shapiro-step Measurement

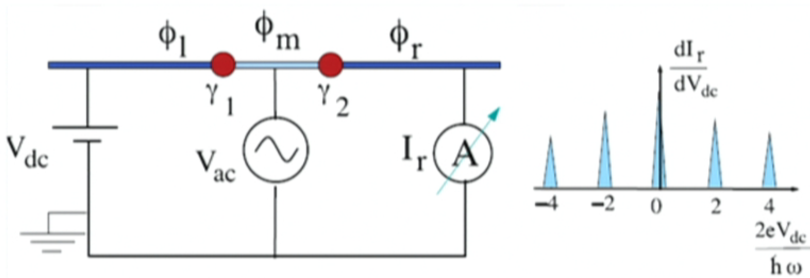

- The new unconventional Josephson current

$$I_Z = \frac{e}{\hbar} J_Z \sin\left(\frac{\phi_l + \phi_r}{2} - \phi_m\right)$$

- It has unique features in three-leg Shapiro-step measurement. For $\phi_l = \frac{2eV_{dc}t}{\hbar}$, $\phi_m = -\left(\frac{2eV_{ac}}{\hbar\omega}\right) cos\omega t$, a current measurement on the right lead will find Shapiro steps emerging only when

$$\frac{2eV_{dc}}{\hbar} = \mathbf{2}n\,\omega$$

- Different from the conventional Shapiro steps $\frac{2eV_{dc}}{\hbar} = n\omega$

L.J., D. Pekker, J. Alicea, G. Refael, Y. Oreg and F. von Oppen, PRL (Accepted) *arXiv: 1107.4102*.

Some Future Directions

Topologically Protected Edge Modes for QST

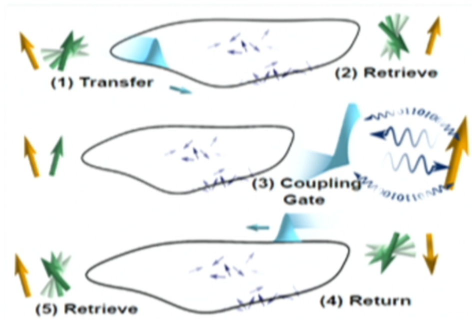

Optically Connected Topological Quantum Networks

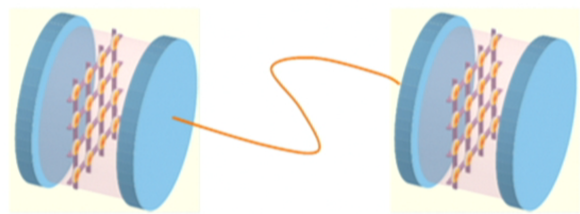

Spintronics in Quantum Wires

$$H = p\sigma^z\tau^z - \mu\tau^z + \Delta(\tau^x\cos\phi - \tau^y\sin\phi) + B_\perp(\sigma^x\cos\theta - \sigma^y\sin\theta)$$

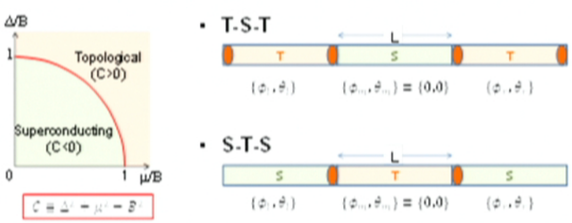

- Without loss of generality, we may fix $\{\phi_m, \theta_m\} = \{0,0\}$.
- Given parameters of L and $\{B, \Delta\}$ for all three regions, the coupling energy is $E = E(\phi_1, \phi_2, \theta_1, \theta_2)$.

Single Molecule MRI

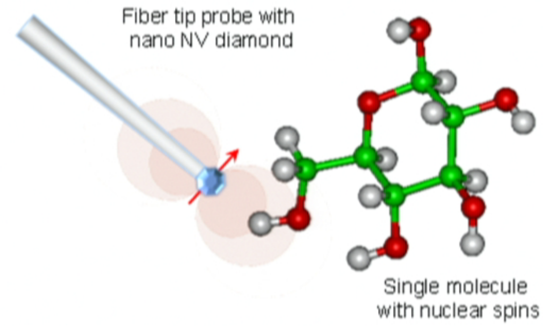

Summary of Other Results

Three-leg Shapiro-step Measurement

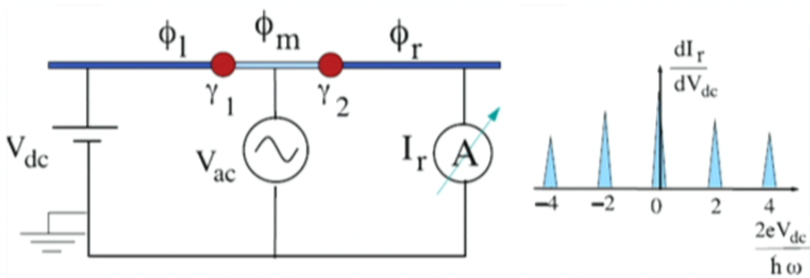

- The new unconventional Josephson current

$$I_Z = \frac{e}{\hbar} J_Z \sin\left(\frac{\phi_l + \phi_r}{2} - \phi_m\right)$$

- It has unique features in three-leg Shapiro-step measurement. For $\phi_l = \frac{2eV_{dc}t}{\hbar}$, $\phi_m = -\left(\frac{2eV_{ac}}{\hbar\omega}\right) cos\omega t$, a current measurement on the right lead will find Shapiro steps emerging only when

$$\frac{2eV_{dc}}{\hbar} = \mathbf{2}n\,\omega$$

- Different from the conventional Shapiro steps $\frac{2eV_{dc}}{\hbar} = n\omega$

L.J., D. Pekker, J. Alicea, G. Refael, Y. Oreg and F. von Oppen, PRL (Accepted) *arXiv: 1107.4102*.